iScience

CellPress
OPEN ACCESS

Article

Anti-angiogenic collagen IV-derived peptide target engagement with $\alpha_v\beta_3$ and $\alpha_5\beta_1$ in ocular neovascularization models

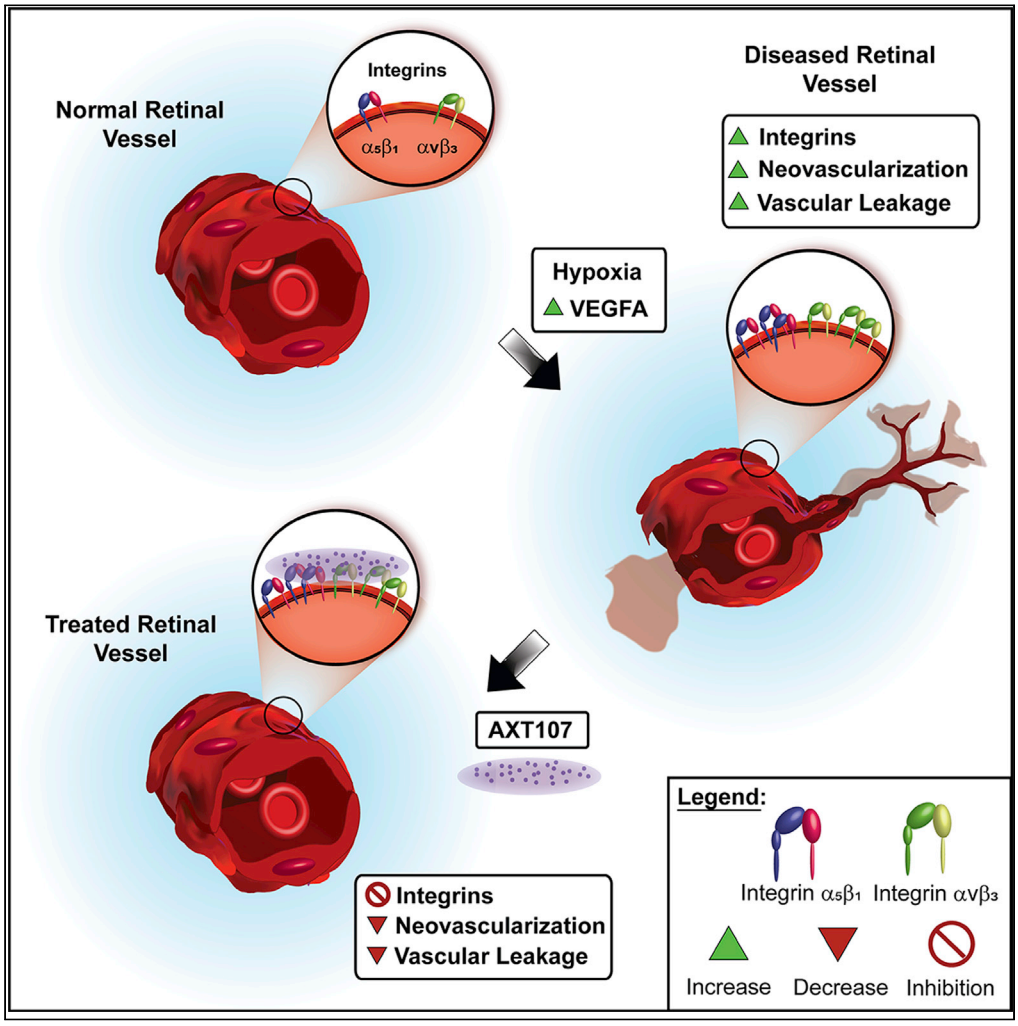

Raquel Lima e Silva, Adam C. Mirando, Stephany Y. Tzeng, Jordan J. Green, Aleksander S. Popel, Niranjan B. Pandey, Peter A. Campochiaro

pcampo@jhmi.edu

Highlights

Expression of integrins $\alpha_v\beta_3$ and $\alpha_5\beta_1$ is increased on pathologic retinal vessels

AXT107 peptide and integrins $\alpha_v\beta_3$ and $\alpha_5\beta_1$ co-localize on pathologic retinal vessels

AXT107-integrin interactions occur predominantly at cell-cell junctions

AXT107 peptide cross-links with integrins $\alpha_v\beta_3$ and $\alpha_5\beta_1$ in hypoxic retinas

Lima e Silva et al., iScience 26, 106078
February 17, 2023
https://doi.org/10.1016/j.isci.2023.106078

iScience

CellPress
OPEN ACCESS

Article

Anti-angiogenic collagen IV-derived peptide target engagement with $\alpha_v\beta_3$ and $\alpha_5\beta_1$ in ocular neovascularization models

Raquel Lima e Silva,[1,2,6] Adam C. Mirando,[3,4,6] Stephany Y. Tzeng,[4,5] Jordan J. Green,[1,4,5] Aleksander S. Popel,[4] Niranjan B. Pandey,[3,4] and Peter A. Campochiaro[1,2,7,*]

SUMMARY

AXT107, a collagen-derived peptide that binds integrins $\alpha_v\beta_3$ and $\alpha_5\beta_1$ with high affinity, suppresses vascular endothelial growth factor (VEGF) signaling, promotes angiopoietin 2-induced Tie2 activation, and suppresses neovascularization (NV) and vascular leakage. Immunohistochemical staining for $\alpha_v\beta_3$ and $\alpha_5\beta_1$ was markedly increased in NV compared with normal retinal vessels. After intravitreous injection of AXT107, there was no staining with an anti-AXT107 antibody on normal vessels but robust staining of NV that co-localized with $\alpha_v\beta_3$ and $\alpha_5\beta_1$. Likewise, after intravitreous injection, fluorescein amidite-labeled AXT107 co-localized with $\alpha_v\beta_3$ and $\alpha_5\beta_1$ on NV but not normal vessels. AXT107 also co-localized with α_v and α_5 at cell-cell junctions of human umbilical vein endothelial cells (HUVECs). AXT107-integrin binding was demonstrated by *ex vivo* cross-linking/pull-down experiments. These data support the hypothesis that AXT107 therapeutic activity is mediated through binding $\alpha_v\beta_3$ and $\alpha_5\beta_1$ which are markedly up-regulated on endothelial cells in NV providing selective targeting of diseased vessels which has therapeutic and safety benefits.

INTRODUCTION

Retinal/choroidal vascular diseases are prevalent causes of visual disability and blindness. Two particularly common diseases that fall into this category are age-related macular degeneration (AMD) and diabetic retinopathy.[1,2] The eyes of patients with AMD have deposits under the retinal pigmented epithelium (RPE) associated with slowly progressive degeneration of the RPE and photoreceptors in the macula often causing gradual loss of central vision over many years or decades.[3] About 10% of patients with AMD develop neovascular AMD (nAMD) in which there is neovascularization (NV) originating from the choroid or deep retinal capillary bed that invades the subretinal space and leaks fluid into the macula causing rapid reduction of vision. Drop out of choroidal vessels which is likely to cause hypoxia of the outer retina has been shown in postmortem eyes from patients with AMD.[4,5] In eyes of patients with diabetic retinopathy, hyperglycemia damages retinal vessels causing slowly progressive vessel closure and progressive retinal ischemia over many years.[6] When a critical threshold of retinal ischemia is exceeded, retinal NV and/or excessive retinal vascular leakage occur. Retinal NV can be complicated by vitreous hemorrhage, traction retinal detachment, and severe loss of vision. Leakage from retinal vessels in the macula causes macular edema and moderate or severe vision loss.

Elucidation of the molecular pathogenesis of retinal/choroidal vascular diseases is critical for the development of therapies. A major step forward has been the demonstration that stabilization of hypoxia-inducible factor-1 (HIF-1) promotes subretinal NV like that seen in nAMD and retinal NV and like that seen in proliferative diabetic retinopathy.[7–11] Increased production of the hypoxia-stimulated gene product, vascular endothelial growth factor-A (VEGFA), is an important stimulus in nAMD, diabetic macular edema, and proliferative diabetic retinopathy, and intraocular injections of VEGF antagonists provide substantial benefit in each.[12] Angiopoietin 2 is a second hypoxia-regulated gene product that has been implicated in retinal/choroidal NV,[13–15] and data from clinical trials suggest that its suppression may provide benefit.[16–18]

One strategy to identify additional molecular targets has been to study endogenous proteins that display anti-angiogenic activity. Sequences common to several anti-angiogenic proteins were used as a starting point to design peptides that were tested for anti-angiogenic activity.[19] Several peptides derived from

[1]Department of Ophthalmology and The Wilmer Eye Institute, Johns Hopkins University School of Medicine, Baltimore, MD, USA

[2]Department of Neuroscience, Johns Hopkins University School of Medicine, Baltimore, MD, USA

[3]AsclepiX Therapeutics, Inc., Baltimore, MD, USA

[4]Department of Biomedical Engineering, Johns Hopkins University School of Medicine, Baltimore, MD, USA

[5]Translational Tissue Engineering Center, Johns Hopkins University School of Medicine, Baltimore, MD, USA

[6]These authors contributed equally

[7]Lead contact

*Correspondence: pcampo@jhmi.edu

https://doi.org/10.1016/j.isci.2023.106078

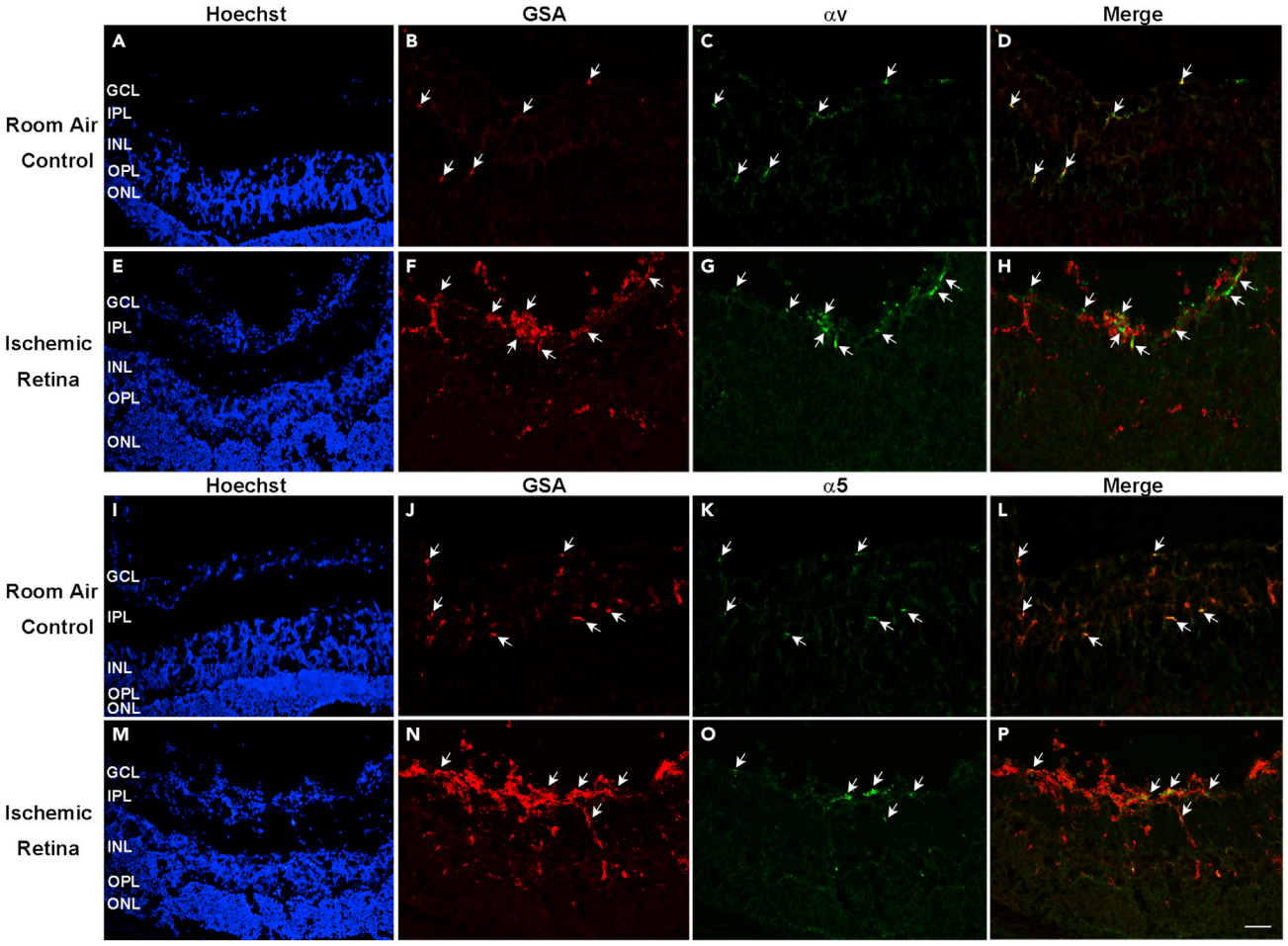

Figure 1. Integrin monomers α_v and α_5 are detected in blood vessels in normal retina and in neovascularization in ischemic retina

At P17, ocular frozen sections from normal C57BL/6 mice (n = 10, A–D and I–L) or from mice with oxygen-induced retinopathy (n = 10, E–H and M–P) were stained with Alexa Fluor 594-conjugated *Griffonia Simplicifolia* Agglutinin (GSA) lectin that selectively stains vascular cells and immunostained for αv and α5. A minimum of 20 ocular sections were assessed per group. The study was replicated, and it showed qualitatively similar result each time. Scale bar = 100 μm.

collagen IV showed anti-angiogenic activity[20] and led to the synthesis of a 20-mer peptide, AXT107, which strongly suppresses retinal and choroidal NV.[21] AXT107 binds integrins $\alpha_v\beta_3$ and $\alpha_5\beta_1$, which have been implicated in NV.[22–26] Integrin $\alpha_v\beta_3$ acts as a co-receptor for VEGFR2 and antibodies that bind it reduce VEGF signaling.[27–29] AXT107 suppresses VEGF signaling and reduces levels of VEGFR2 in cultured vascular endothelial cells, providing indirect evidence that its binding of $\alpha_v\beta_3$ contributes to its anti-angiogenic activity.[21] Integrin $\alpha_5\beta_1$ interacts with Tie2 to sensitize its activation by angiopoietin 1.[30,31] AXT107 causes dissociation of $\alpha_5\beta_1$ and strongly stimulates Tie2 activation in the presence of angiopoietin 2 in cultured endothelial cells.[32] Tie2 activation by other mechanisms suppresses ocular NV and reduces excessive vascular permeability[33–35] suggesting that AXT107-induced Tie2 activation through its interaction with $\alpha_5\beta_1$ may also contribute to suppression of vascular leakage and NV. To further test the hypothesis that the mechanism of therapeutic activity of AXT107 in animal models of ocular NV is through binding integrins $\alpha_v\beta_3$ and $\alpha_5\beta_1$, we tested for engagement of AXT107 with these targets in animal models of ocular NV in which it exerts therapeutic benefit.

RESULTS

Integrins α_v and α_5 are present in vessels in normal retina and NV in ischemic retina

Alexa Fluor 594-conjugated *Griffonia Simplicifolia* Agglutinin (GSA) lectin stains vascular cells, and in ocular sections from normal P17 C57BL/6 mice, it stains segments of retinal blood vessels throughout the inner retina (Figures 1A and 1B, arrows). Immunostaining with an antibody that specifically recognizes integrin

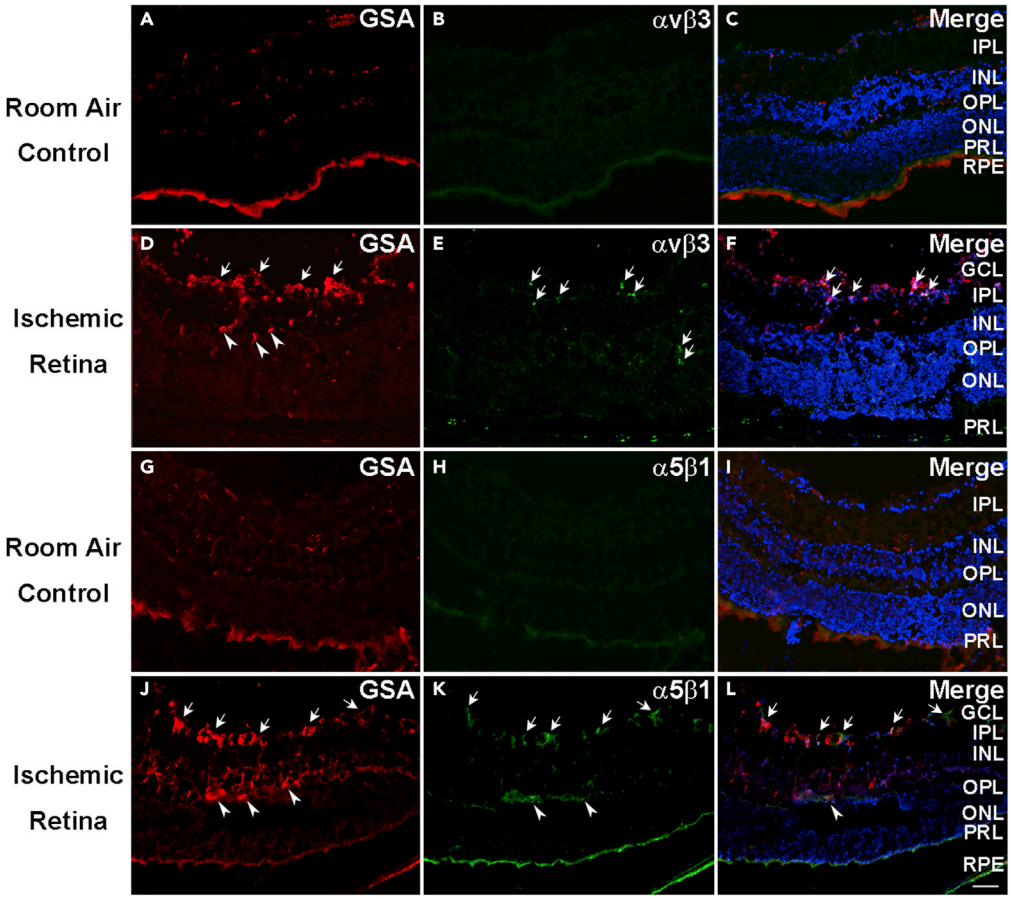

Figure 2. Integrins $\alpha_v\beta_3$ and $\alpha_5\beta_1$ are upregulated in neovascularization and some pre-existent retinal vessels in ocular sections of ischemic retina

At P17, C57BL/6 room air control mice (n = 10) or mice with oxygen-induced ischemic retinopathy (n = 10, OIR) were euthanized and ocular sections were stained with Alexa Fluor 594-conjugated *Griffonia Simplicifolia* Agglutinin (GSA) lectin and immunostained for $\alpha_v\beta_3$ or $\alpha_5\beta_1$. There was no $\alpha_v\beta_3$ detectable on GSA-labeled retinal vessels in room air control retina (A–C), but it was detectable in NV and pre-existent vessels in ischemic retina ocular sections from P17 mice with OIR (D–F). Similarly, integrin $\alpha_5\beta_1$ was not detectable on GSA-labeled retinal vessels in room air control retina (G–I), but it was detectable in NV and pre-existent vessels in ocular sections (J–L) from mice with OIR. A minimum of 20 ocular sections were assessed per group. The study was replicated, and it showed qualitatively similar result each time. Scale bar = 100 μm.

α_v showed staining for α_v in GSA-labeled vessel segments (Figures 1C and 1D). In mice with oxygen-induced ischemic retinopathy (OIR), a model that mimics aspects of retinopathy of prematurity and proliferative diabetic retinopathy,[36] GSA-labeled NV on the surface of the retina also stained for integrin α_v (Figures 1E–1H). Similarly, there was staining for α_5 in blood vessels in normal retina and in NV and feeder vessels in retinas from mice with OIR (Figures 1I–1P).

Integrins $\alpha_v\beta_3$ and $\alpha_5\beta_1$ are upregulated on blood vessels and NV in ischemic retina

Immunostaining with an antibody directed against integrin heterodimer $\alpha_v\beta_3$ showed no staining of retinal vessels in ocular sections of P17 room air control mice with normal retinas (Figures 2A–2C) but showed staining of NV and pre-existent vessels in P17 OIR retina (Figures 2D–2F). The situation was similar for integrin $\alpha_5\beta_1$, which was undetectable on retinal vessels in normal P17 retina (Figures 2G–2I) but was present in NV and pre-existent retinal vessels in ischemic retina (Figures 2J–2L). There was no detectable staining for $\alpha_v\beta_3$ in retinal flat mounts from P17 room air control mice (Figures 3A–3C), but GSA-labeled buds of NV on the surface of retinas from OIR mice stained for $\alpha_v\beta_3$ (Figures 3D–3F). Similarly, staining for α5β1 was not detectable in retinal flat mounts from P17 room air control mice (Figures 3G–3I), but stained NV on the surface of retinas from P17 OIR mice was detected (Figures 3J–3L).

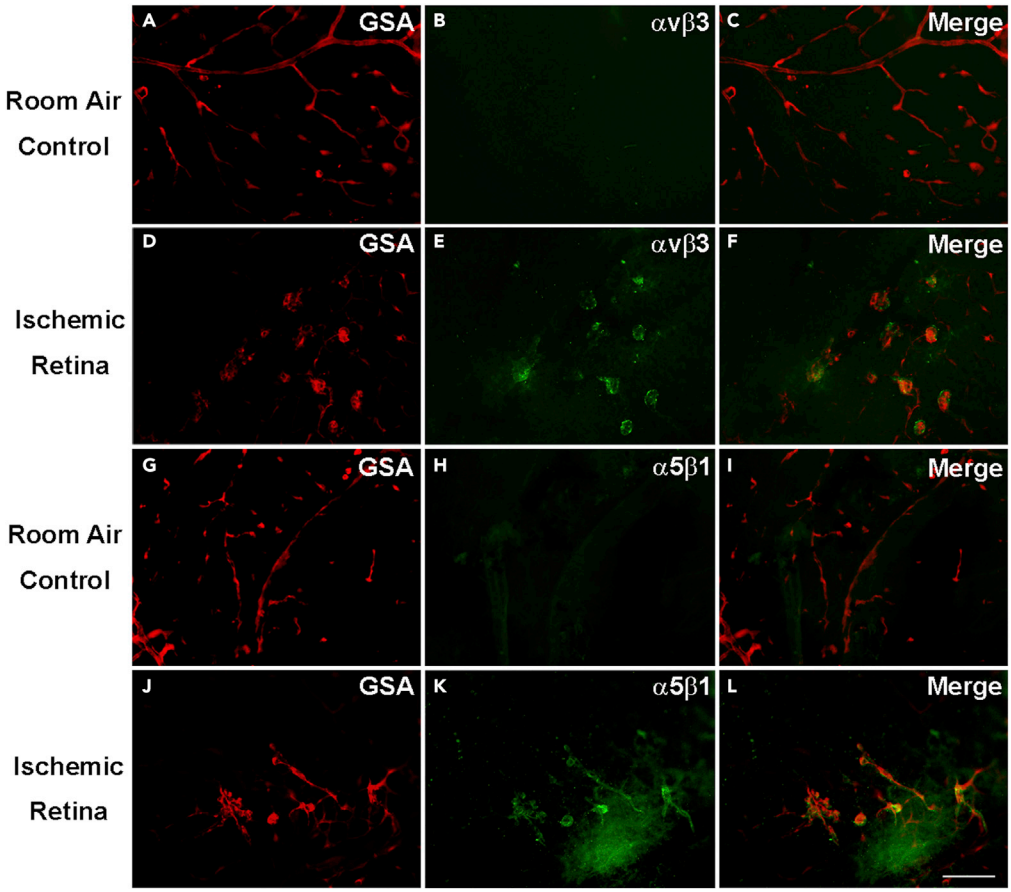

Figure 3. Integrins $\alpha_v\beta_3$ and $\alpha_5\beta_1$ are upregulated in neovascularization in flat mounts of ischemic retina

At P17, C57BL/6 room air control mice (n = 10) or mice with oxygen-induced ischemic retinopathy (n = 10, OIR) were euthanized and retinal flat mounts were stained with Alexa Fluor 594-conjugated *Griffonia Simplicifolia* Agglutinin (GSA) lectin and immunostained for $\alpha_v\beta_3$ or $\alpha_5\beta_1$. There was no $\alpha_v\beta_3$ detectable on GSA-labeled retinal vessels in room air control retina (A–C), but it was detectable in buds of NV on retinal flat mounts from P17 mice with OIR (D–F). Similarly, integrin $\alpha_5\beta_1$ was not detectable on GSA-labeled retinal vessels in room air control retina (G–I), but it was detectable in NV in retinal flat mounts (J–L) from mice with OIR. The experiment was performed in duplicates, and qualitatively similar results were found in the replicates. Scale bar = 100 μm.

Primary antibody controls are shown in Figure S1. At P17, C57BL/6 mice with OIR and *rho/VEGF* transgenic mice at P21 were euthanized, and ocular sections were immunohistochemically stained with Alexa Fluor 594-labeled GSA or fluorescein isothiocyanate (FITC)-GSA and secondary anti-rabbit immunoglobulin G (IgG) (Figures S1A–S1F) or anti-rat IgG (Figures S1G–S1L). There was no staining in the absence of primary antibodies as shown in representative images of OIR mice (Figures S1A–S1C and S1G–S1I) or *rho/VEGF* transgenic mice (Figures S1D–S1F and S1J–S1L).

AXT107 co-localizes with α_v and α_5 integrins in HUVEC monolayers

Epifluorescence microscopy at 200× magnification revealed a diffuse immunohistochemical signal for α_5 integrin on the surface of cultured HUVECs and no signal in the green channel (Figures S2A–S2C). After addition of fluorescein amidite (FAM)-labeled AXT107, immunostaining of the cells with anti-α_5 antibody showed co-localization of AXT107 with α_5 integrin (Figures S2D–S2F). Similarly, there was diffuse staining for α_v integrin on the surface of HUVECs (Figures S2G–S2I). After addition of FAM-labeled AXT107, immunostaining with anti-α_v antibody showed co-localization of AXT107 and α_v integrin (Figures S2J–S2L). The localization of FAM-AXT107 was further resolved by z series confocal imaging of cultured HUVECs at 630× magnification and 0.3 μm step size. Consistent with the epifluorescence results, FAM-AXT107 appeared to co-localize with both integrins α_5 (Figures 4A–4C) and α_v (Figures 4D–4F). The higher resolution further revealed that the peptide concentrated at the bottom of the well at the

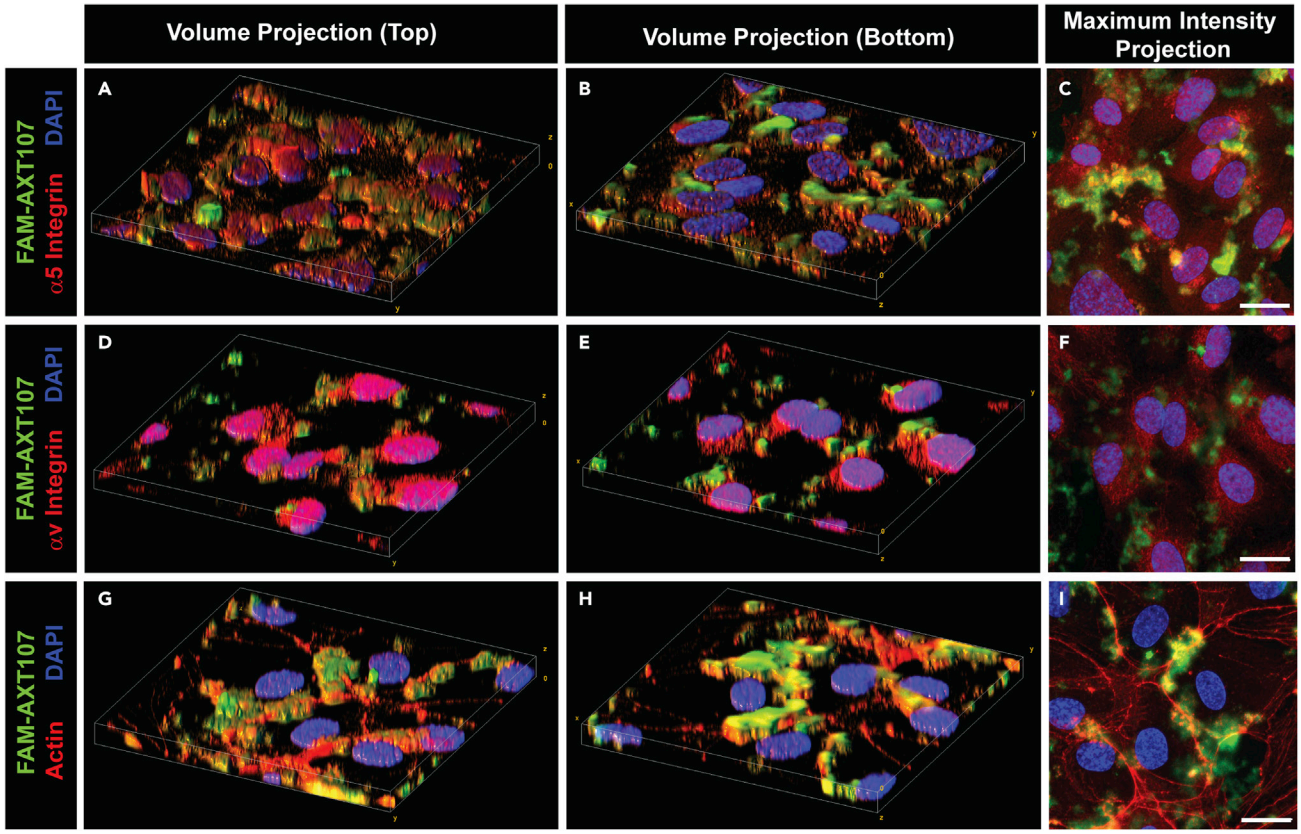

Figure 4. AXT107 co-localizes with α_5 and α_v integrins at cell-cell junctions in cultured human umbilical vein endothelial cell (HUVEC) monolayers

HUVEC monolayers were treated with 25 μM AXT107 containing 25% fluorescein amidite (FAM)-labeled AXT107 (green) and then immunohistochemically stained with antibodies against integrins α_5 (A–C) or α_v (D-F) or F-actin using rhodamine-phalloidin (G–I) (red). DAPI (blue) was included as a nuclear stain in all images. Images were taken as z series using the 63× objective and 0.3 μm step sizes. Data are presented as merged volume projections at an angle from both the top (A, D, and G) and the bottom (B, E, and H) and as a maximum intensity projection (C, F, and I). N = 2; Scale bar = 20 μm.

cell-plate interface rather than the apical surface of the cell body and does not appear to be taken up into the cells. Moreover, the elongated appearance and distance of the FAM-AXT107 signal from the nuclei suggested that the peptide could be localizing to intercellular junctions. The junctional localization was subsequently confirmed by showing co-localization of FAM-AXT107 with actin (Figures 4G–4I), which was previously shown to redistribute to endothelial cell junctions upon treatment with AXT107.[32]

Anti-AXT107 antibody specifically stains AXT107

Dot blot of AXT107 in water, SDS buffer, or HUVEC lysates showed concentration-dependent staining of AXT107 with anti-AXT107 antibody (Figure S3A). Addition of FAM-labeled AXT107 (FAM-AXT107) to HUVEC monolayers followed by immunohistochemical staining with anti-AXT107 antibody showed co-localization of FAM-AXT107 and antibody-stained AXT107 (Figure S3B).

After intravitreous injection of AXT107 in mice with OIR, AXT107 is localized in retinal NV

Staining of the retina from a P17 room air control mouse with the antibody directed against AXT107 showed no signal as expected (Figures 5A–5C). At P16, mice with OIR were given an intravitreous injection of AXT107 or PBS, and after one day, ocular sections showed GSA-labeled NV on the retinal surface (Figure 5D) that immunohistochemically stained for AXT107 (Figures 5E and 5F). In PBS-injected animals, there was no signal in the green channel within the retina (Figures 5G–5I). Retinal flat mounts of AXT107-injected eyes from P17 OIR mice showed strong staining for AXT107 in GSA-labeled NV (Figures 5J–5L) but not in eyes of P17 OIR mice that had been injected with PBS (Figures 5M–5O).

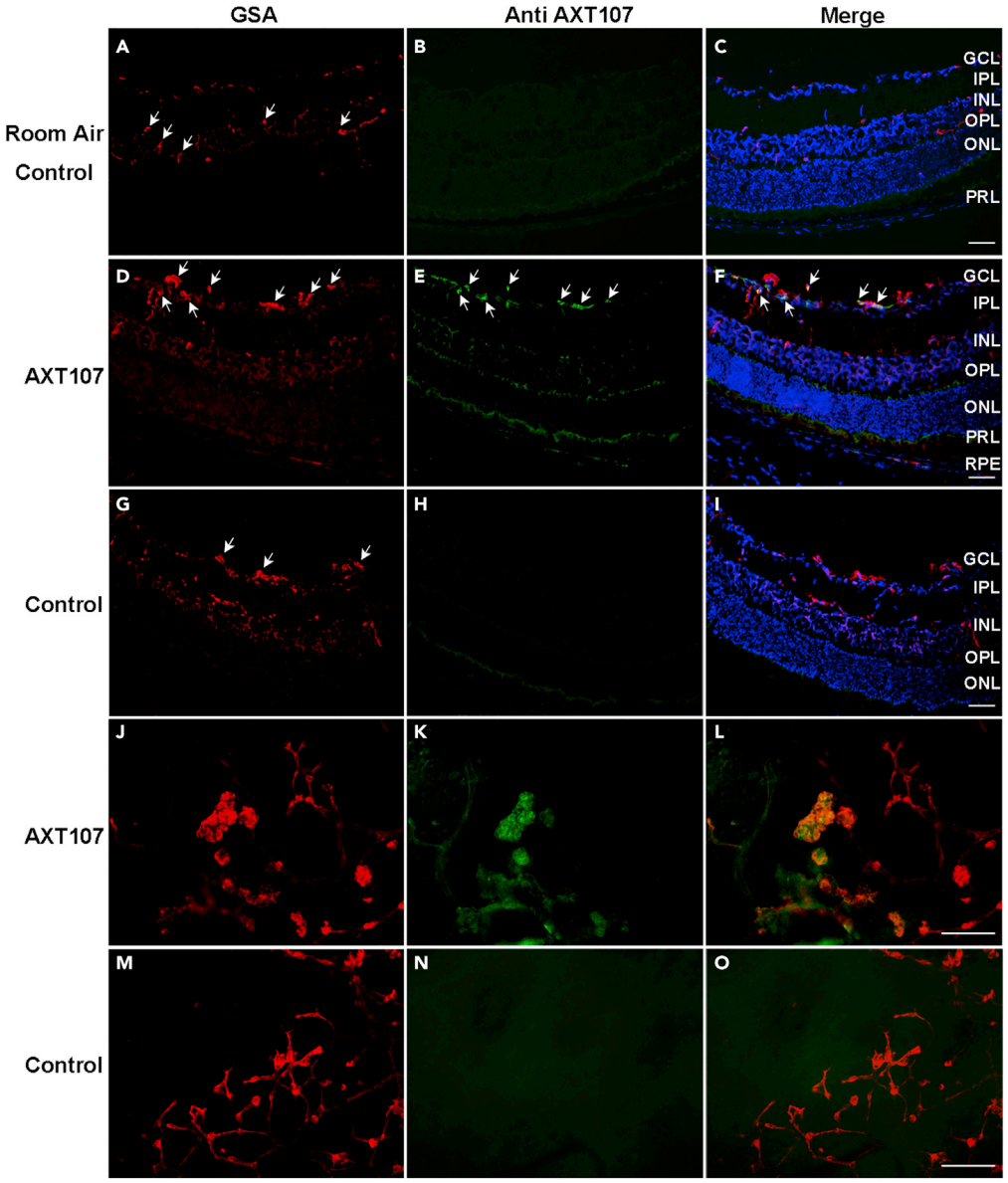

Figure 5. After intraocular injection, AXT107 was localized within retinal neovascularization (NV) in ischemic retina

At P16, room air control mice (n = 10) or mice with oxygen-induced ischemic retinopathy (n = 10, OIR) were given an intravitreous injection of 1 μg of AXT107 in one eye and PBS in the fellow eye. After 24 h, ocular sections or retinal flat mounts were stained with Alexa Fluor 594-conjugated *Griffonia Simplicifolia* Agglutinin (GSA) lectin and immunostained for AXT107. AXT107 was not detected in the retinas of room air control mice 24 h after intravitreous injection of AXT107 (A–C), but it was seen within GSA-labeled NV in ocular sections (D–F) and retinal flat mounts (J–L) of mice with OIR. There was no staining for AXT107 in the retinas of PBS-injected eyes of mice with OIR (G–I and M–O). A minimum of 20 ocular sections were assessed per group. The study was conducted in duplicates, and qualitatively similar results were found in the replicates. Scale bars = 100 μm.

After intraocular injection, AXT107 localizes to type 3 choroidal NV in which cells stain for $\alpha_v\beta_3$ and $\alpha_5\beta_1$

In *rho/VEGF* transgenic mice, the *rhodopsin* promoter drives expression of $VEGF_{165}$ in photoreceptors resulting in NV that grows from the deep capillary bed of the retina into the subretinal space.[37,38] This type of NV, referred to as retinal angiomatous proliferation or type 3 choroidal NV, is seen in roughly 30% of patients with nAMD.[39] Intraocular injection of AXT107 strongly suppresses type 3 choroidal NV in *rho/VEGF*

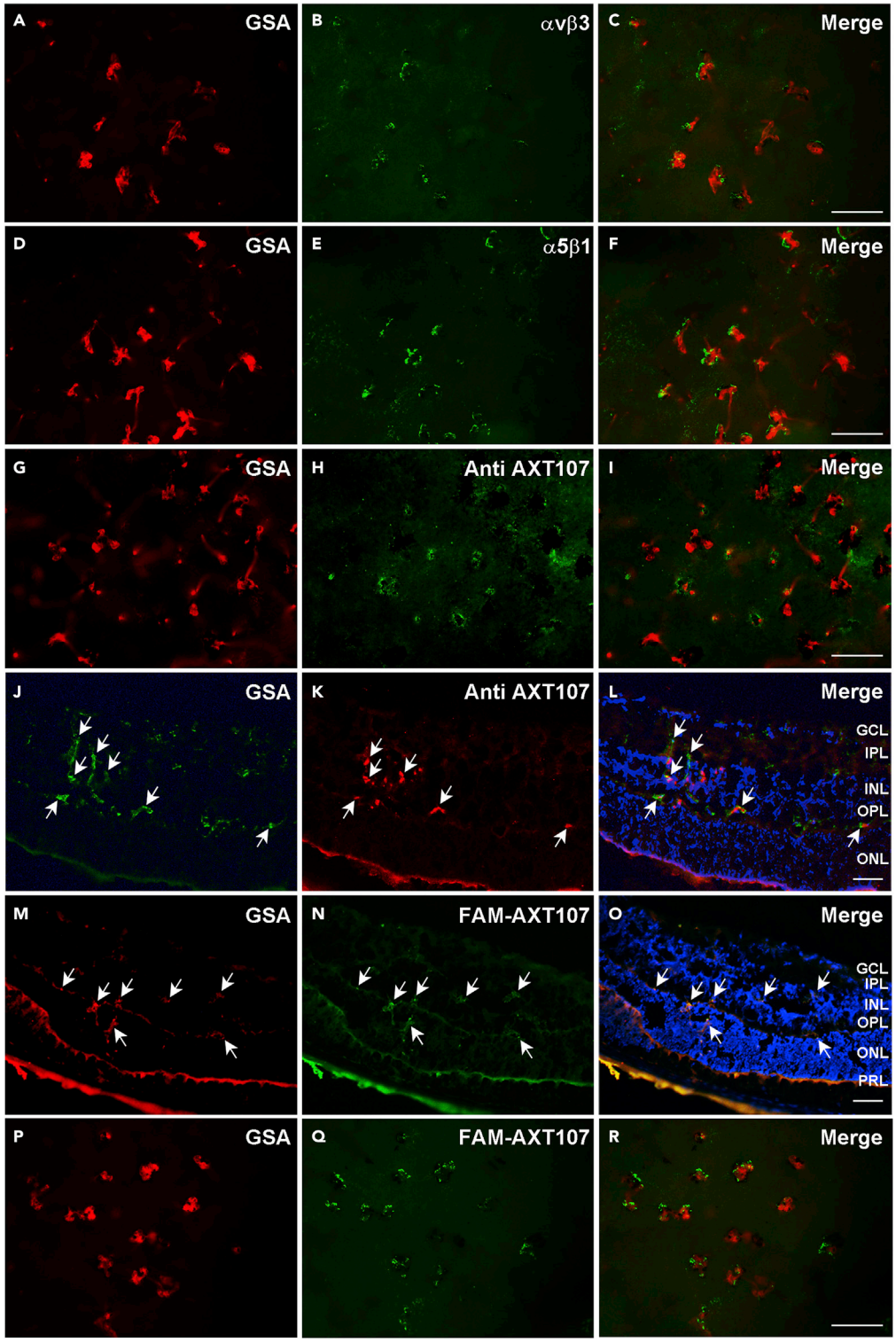

Figure 6. After intraocular injection, AXT107 localizes to type 3 choroidal neovascularization (NV) in which cells stain for $\alpha_v\beta_3$ and $\alpha_5\beta_1$

At P20, *rho/VEGF* mice were given an intravitreous injection of 1 μg of AXT107 (n = 10, A-L) or FAM-labeled AXT107 (n = 10, M-R). After 24 h retinal flat mounts or ocular sections were stained with FITC-*Griffonia Simplicifolia* Agglutinin (GSA) lectin (A and J) or Alexa Fluor 594-GSA (D, G, M, and P). Retinal flat mounts immunostained for $\alpha_v\beta_3$ (A–C), $\alpha_5\beta_1$ (D–F) or

Figure 6. *Continued*
AXT107 (G–I), showed staining for each within GSA-labeled buds of NV. Ocular sections also showed FITC-GSA-labeled NV that immunostained for AXT107 (J–L). Ocular sections (M–O) and retinal flat mounts (P–R) from eyes of P21 *rho/VEGF* mice that had been given an intravitreous injection of 1 μg of fluorescein amidite (FAM)-labeled AXT107 24 h before showed FAM-AXT107 in close association with Alexa Fluor 594-GSA-labeled type 3 choroidal NV (O and R). The study was conducted in duplicates, and qualitatively similar results were found in the replicates. Scale bars = 100 μm.

mice.[21] Twenty-four hours after intravitreous injection of 1 μg of AXT107 in eyes of P20 *rho/VEGF* mice, retinal flat mounts showed immunostaining for $\alpha_v\beta_3$ (Figures 6A–6C) and $\alpha_5\beta_1$ (Figures 6D–6F) in NV on the outer surface of the retina. There was also immunostaining for AXT107 in and around NV on the outer surface of retinal flat mounts (Figures 6G–6I) and vessels within the retina seen in ocular sections (Figures 6J–6L). Twenty-four hours after intravitreous injection of FAM-AXT107 in P20 *rho/VEGF* mice, ocular sections and retinal flat mounts showed FAM-AXT107 in and around NV in the outer retina and on the outer surface of the retina (Figures 6M–6O and 6P–6R, respectively). In contrast, 24 h after injection of FAM-AXT107 in P20 wild-type mice, there was no fluorescence seen in the retina (Figures S4A–S4D). Three days after intravitreous injection of FAM-AXT107 in P14 mice with OIR and P18 *rho/VEGF* mice, ocular sections still showed positive FAM-AXT107 stain in and around NV on the outer surface of the retina (Figures S4E–S4H and S4I–S4L, respectively). The suppression of NV at longer time points after AXT107 precludes assessing the localization of AXT107 at time points beyond 3 days after injection.

Integrins $\alpha_v\beta_3$ and $\alpha_5\beta_1$ co-localize with AXT107 in ischemic retina and type 3 choroidal NV

Twenty-four hours after P16 OIR mice were given an intravitreous injection of 1 μg of AXT107, immunostaining of ocular sections showed co-localization of $\alpha_v\beta_3$ and AXT107 (Figures 7A–7D) and co-localization of $\alpha_5\beta_1$ and AXT107 (Figures 7E–7H). Twenty-four hours after a 1 μg injection of AXT107 in P20 *rho/VEGF* transgenic mice, immunostaining of ocular sections showed co-localization of AXT107 with $\alpha_v\beta_3$ (Figures 7I–7L).and $\alpha_5\beta_1$ (Figures 7M–7P). Twenty-four hours after a 1 μg injection of AXT107 in C57BL/6 wild-type control mice, there was no detectable staining for $\alpha_v\beta_3$ or AXT107(Figures 7Q–7T) and no detectable staining for $\alpha_5\beta_1$ or AXT107 (Figures 7U–7X).

After intravitreous injection, AXT107 co-localizes with $\alpha_v\beta_3$ and $\alpha_5\beta_1$ in choroidal NV

Adult C57BL/6 mice with laser-induced rupture of Bruch's membrane develop NV that grows from the choroid into the subretinal space.[40] This is referred to as type 2 choroidal NV and is the predominant type of NV in patients with nAMD. Intraocular injection of AXT107 in mice with laser-induced rupture of Bruch's membrane also strongly suppresses type 2 choroidal NV, which is best visualized on eyecup flat mounts in which the NV is seen as vessels growing on the surface of the RPE in a circular pattern.[21] Adult C57BL/6 mice were given an intravitreous injection of 1 μg of AXT107 six days after laser-induced rupture of Bruch's membrane and euthanized 24 h later. After removal of the retina, flat mounts of eyecups showed diffuse GSA labeling of type 2 choroidal NV at Bruch's membrane rupture sites with overlapping more focal immunostaining for $\alpha_v\beta_3$ (Figures 8A–8C), $\alpha_5\beta_1$ (Figures 8D–8F), and AXT107 (Figures 8G–8I). There was no staining for AXT107 in PBS-injected eyes (Figures 8J–8L). AXT107 co-localized with $\alpha_v\beta_3$ (Figures 8M–8O) and $\alpha_5\beta_1$ (Figures 8P–8R) with choroidal NV. Ocular frozen sections 7 days after laser-induced rupture of Bruch's membrane and 1 day after intravitreous injection of 1 μg of AXT107 showed immunostaining for $\alpha_v\beta_3$ (Figures S5A–S5D) and $\alpha_5\beta_1$ (Figures S5E–S5H) and localization of AXT107 (Figures S5I–S5L) within choroidal NV. When PBS was injected instead of AXT107 after rupture of Bruch's membrane, there was no staining for AXT107 (Figures S5M–S5P). Seven days after rupture of Bruch's membrane and 1 day after injection of 1 μg of AXT107, there was co-localization of $\alpha_v\beta_3$ and AXT107 (Figures S5Q–S5T) and also co-localization of $\alpha_5\beta_1$ and AXT107 (Figures S5U–S5X) within choroidal NV.

AXT107 binds directly to integrins $\alpha_v\beta_3$ and $\alpha_5\beta_1$ following intraocular injection

To test whether co-localization of AXT107 with $\alpha_v\beta_3$ and $\alpha_5\beta_1$ was due to binding, studies were done using a sulfo-SBED-labeled AXT107 cross-linking approach followed by pull-downs to identify AXT107 binding partners on cell surfaces. A summary of the procedure is outlined in Figure S6. At P16, one set of seven mice reared in room air and two sets of seven OIR mice were injected in both eyes with 1 μg sulfo-SBED-labeled AXT107. The next day, lysates were generated from the pooled retinas of each set following a UV-mediated cross-linking reaction. Integrins α_5, α_V, β1, and β_3 were all present in the lysates (Figures 9A–9D) with integrins α_v and β_3 showing clear induction in OIR mice. Integrins α_5 and β_3, but

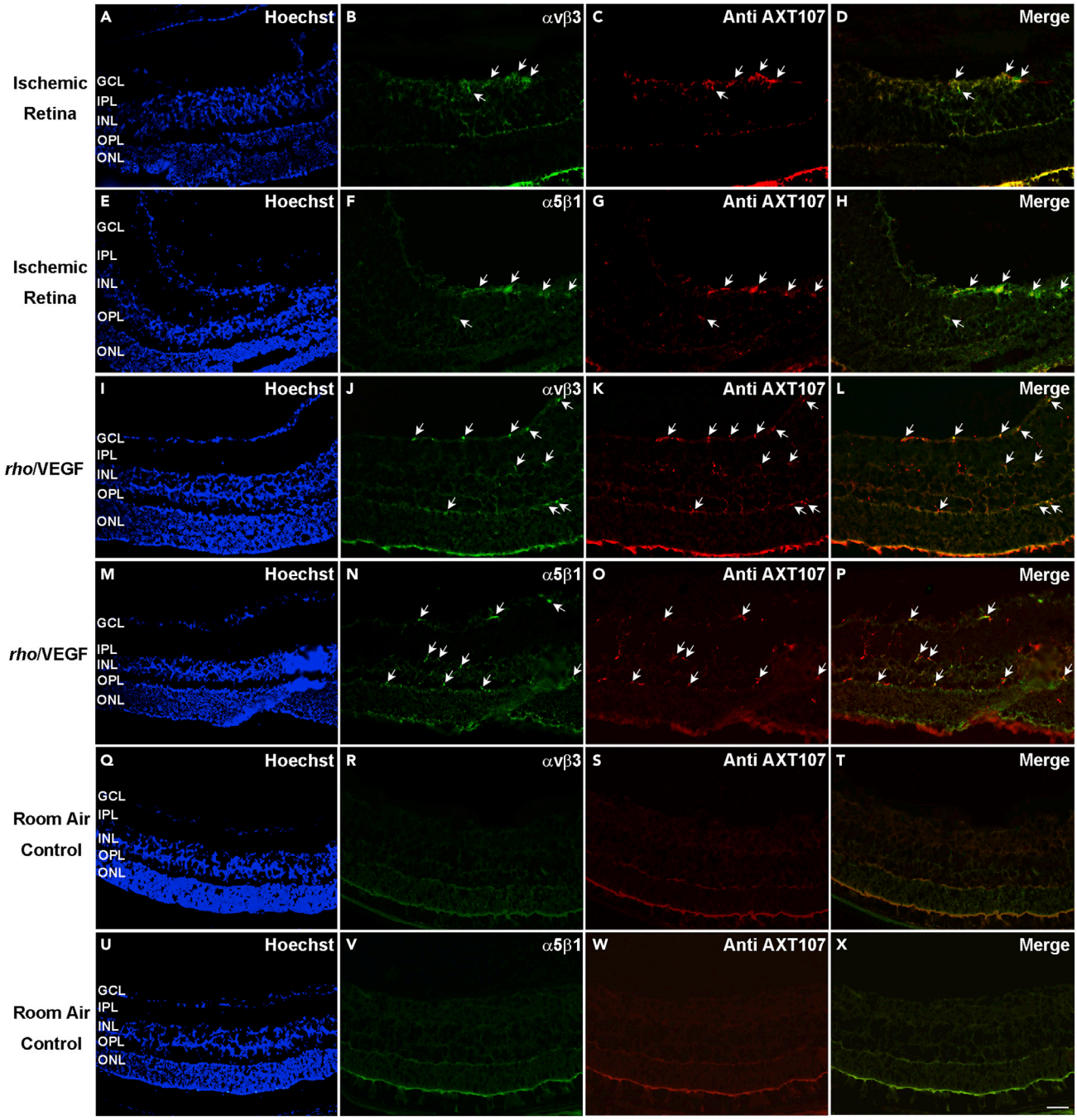

Figure 7. After intraocular injection, AXT107 co-localizes with $\alpha_v\beta_3$ and $\alpha_5\beta_1$ in ischemic retina and retinas of *rho*/VEGF transgenic mice

Mice with oxygen-induced ischemic retinopathy (n = 10, OIR, P16) and *rho/VEGF* transgenic mice (n = 10, P20) were given an intravitreous injection of 1 μg of AXT107. After 24 h, ocular sections were immunostained for $\alpha_v\beta_3$ or $\alpha_5\beta_1$ and AXT107. In the retinas of OIR mice, AXT107 co-localized with $\alpha_v\beta_3$ (A–D) and $\alpha_5\beta_1$ (E–H) in retinal NV on the surface of the retina and in some pre-existent vessels within the retina. In *rho*/VEGF mice, AXT107 co-localized with $\alpha_v\beta_3$ (I–L) and $\alpha_5\beta_1$ (M–P) in vascular structures throughout the retina including type 3 choroidal NV in the outer retina. C57BL/6 wild-type control mice were euthanized, and ocular sections were stained with Alexa Fluor 594-conjugated *Griffonia Simplicifolia* Agglutinin (GSA) lectin and immunostained for $\alpha_v\beta_3$ (n = 10) or $\alpha_5\beta_1$ (n = 10). There was no $\alpha_v\beta_3$ (Q–T) or $\alpha_5\beta_1$ (U–X) detectable on GSA-labeled retinal vessels in room air control retina. A minimum of 20 ocular sections were assessed per group. The study was conducted in duplicates, and qualitatively similar results were found in the replicates. Scale bar = 100 μm.

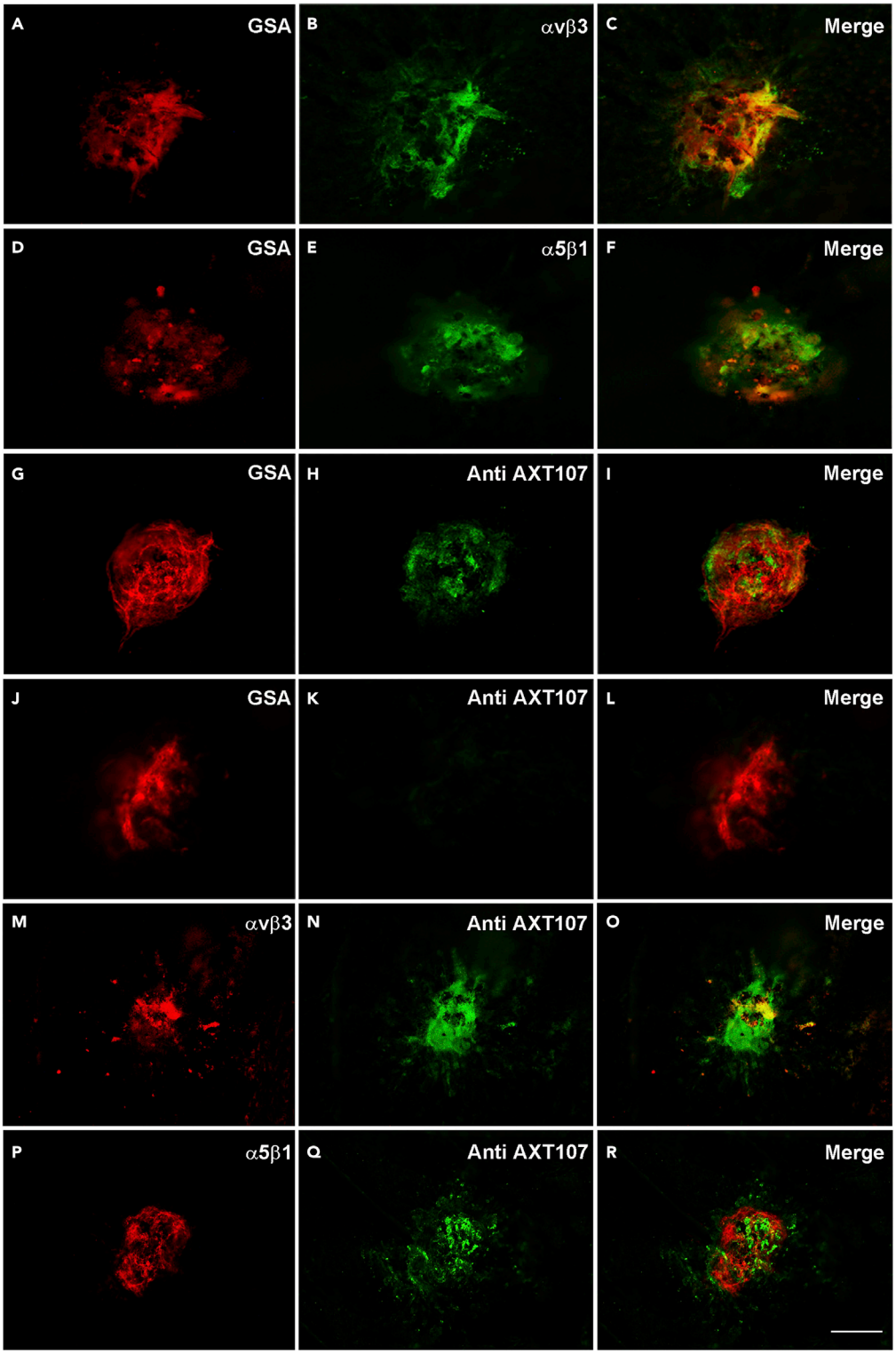

Figure 8. Integrins $\alpha_v\beta_3$ and $\alpha_5\beta_1$ are expressed in cells within type 2 choroidal neovascularization (NV), and after intraocular injection, AXT107 localizes with $\alpha_v\beta_3$ and $\alpha_5\beta_1$

Six days after laser-induced rupture of Bruch's membrane, 10 C57BL/6 mice had intravitreous injection of 1 μg of AXT107 or PBS. After 24 h retinas were removed, and eyecups were stained with Alexa Fluor 594-labeled *Griffonia Simplicifolia* Agglutinin (GSA) lectin and immunostained for $\alpha_v\beta_3$, $\alpha_5\beta_1$, or AXT107. Flat mounts showed GSA labeling throughout

Figure 8. *Continued*
choroidal NV lesions with overlapping focal areas of staining for $\alpha_v\beta_3$ (A–C), $\alpha_5\beta_1$ (D–F) or AXT107 (G–I). Control PBS-injected eyes showed no staining for AXT107 (J–L). In flat mounts stained for AXT107 and $\alpha_v\beta_3$ (M–O) or for AXT107 and $\alpha_5\beta_1$ (P-R), the AXT107 co-localized with each of the integrins. The study was conducted in duplicates, and qualitatively similar results were found in the replicates. Scale bar = 100 μm.

not integrins α_v or β_1, (Figures 9E–9G) were observed after streptavidin-mediated pull-down, suggesting that they cross-linked with AXT107. To demonstrate that these integrin interactions were specific for AXT107, additional cross-linking and pull-down experiments were conducted using sulfo-SBED-labeled SP2048 (sulfo-SBED SP2048), a peptide with a similar sequence to AXT107 (Figure S7A) but reduced inhibitory activity in growth factor signaling pathways associated with integrin $\alpha_v\beta_3$, such as VEGFA/VEGFR2 (Figure S7B), or integrin $\alpha_5\beta_1$, such as HGF/cMet (Figure S7C), or in cell migration assays as reported previously.[41] Pull-down assays of lysates from HUVECs treated with sulfo-SBED SP2048 showed little to no cross-linking with integrins α_5, α_V, β1, or β_3 (Figures S7D–S7G) despite the clear presence of each subunit in the lysates. Dot blot analysis was then used to confirm that the lack of cross-linking was not due to the faulty production of the sulfo-SBED SP2048. While no specific antibody is available for SP2048, the anti-AXT107 antibody was found to cross-react with the SP2048 peptide (Figure S7H). Dot blot analysis of the lysates revealed the complete association of the sulfo-SBED SP2048 with the streptavidin-coated beads (Figure S7I), indicating that all of the observable peptide was successfully labeled.

DISCUSSION

AXT107 is a 20-mer mimetic peptide derived from collagen IV that, when injected into the eye, suppresses retinal and choroidal NV and VEGF-induced vascular leakage.[21] AXT107 binds integrin $\alpha_v\beta_3$ which associates with VEGFR2 and is needed for optimal VEGF signaling. Antibodies directed against α_v subunit or β_3 subunit, but not β_1 subunit, suppress phosphorylation of VEGFR2 in cultured endothelial cells.[27] Incubation of cultured endothelial cells with AXT107 also suppresses phosphorylation of VEGFR2.[21] Because VEGF signaling plays a critical role in growth of NV and excessive vascular leakage in the retina in animal models of retinal vascular disease[42–45] and in clinical trials,[46,47] it is reasonable to conclude that AXT107 suppression of VEGF signaling through $\alpha_v\beta_3$ binding contributes to the inhibition of ocular NV and vascular leakage by AXT107. Likewise, it is reasonable to conclude that binding of AXT107 to $\alpha_5\beta_1$ may also contribute because that binding promotes activation of Tie2,[48] and there is evidence that activation of Tie2 directly or by inhibiting angiopoietin 2 provides benefit in retinal/choroidal vascular diseases.[33–35,49–51]

In this study, the hypothesis that binding of AXT107 to $\alpha_v\beta_3$ and $\alpha_5\beta_1$ contributes to its therapeutic effects in models of retinal/choroidal vascular disease was further strengthened by demonstration that AXT107 engages integrins $\alpha_v\beta_3$ and $\alpha_5\beta_1$ in those disease models. This is complemented by the precise co-localization of AXT107 with α_v and α_5 integrins on HUVECs *in vitro* and cross-linking between integrins sulfo-SBED AXT107 and integrins α_5 and β_3 in *ex vivo* retinas from OIR mice. Regarding specific integrin interactions, the cross-linking experiments clearly show interactions with integrins α_5 and β_3. However, it is still possible that the other subunit of the integrin heterodimer, either β_1 or α_v, is important for the binding of AXT107, either because the interaction occurs at the subunit interface and the cross-link specificity is the result of the sulfo-SBED moiety's orientation at binding or because AXT107 interactions are specific to integrin conformations requiring both subunits to be present. In fact, these possibilities are not mutually exclusive and are supported by findings in this and previous publications. The high-resolution images of AXT107-treated HUVECs in this work indicated that the peptide accumulated at the cellular junctions near the interface of the cells and the culture plate surface, suggesting that the peptide is likely interacting with active integrin heterodimers involved in adhesion to the extracellular matrix. In addition, previous studies of AXT107 revealed that the peptide disrupts integrin $\alpha_5\beta_1$ heterodimers into their individual monomers[32] and directly competes with the binding of antibodies specific to integrins $\alpha_5\beta_1$ and $\alpha_v\beta_3$[21] both of which suggest binding at or near the subunit interface. Despite similarity in sequence, SP2048 did not show the same strong interactions with integrins, indicating that the cross-linking to integrins α_5 and β_3 was peptide specific.

Interestingly, the expression of $\alpha_v\beta_3$ and $\alpha_5\beta_1$ is low in endothelial cells of normal, unstressed retinal vessels and is substantially increased in endothelial cells participating in NV. No association of AXT107 with blood vessels in normal retina was detectable, but a robust association was seen with NV in 3 separate models in which AXT107 co-localized with $\alpha_v\beta_3$ and $\alpha_5\beta_1$ in the NV. This was demonstrated in 2 different ways at 2 time points: (1) immunostaining for the integrins and AXT107 one day after intravitreous injection of unlabeled AXT107 and (2) immunostaining for the integrins three days after intravitreous injection of FAM-labeled

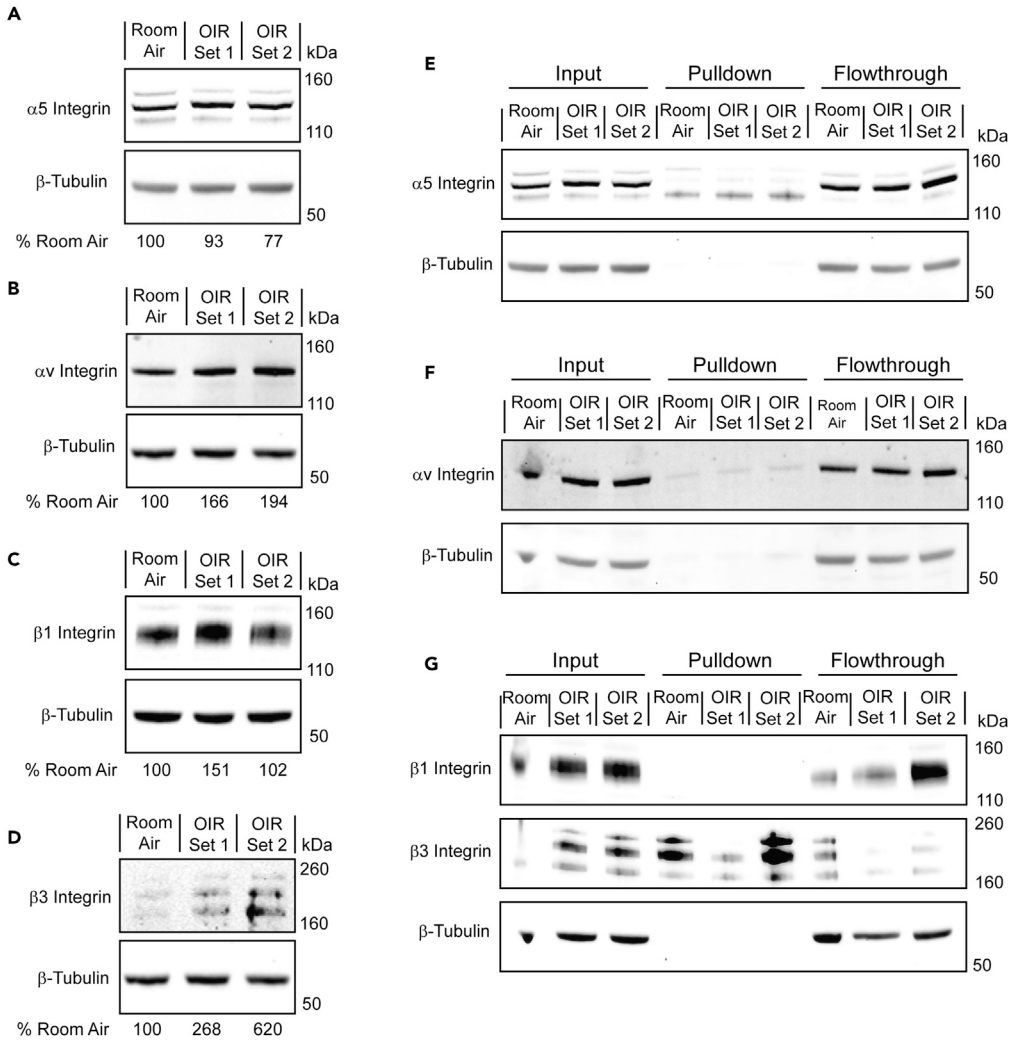

Figure 9. AXT107 cross-links with integrins α_5 and β_3

P16 mice reared in room air (1 set of 7 mice) or OIR (2 sets of 7 mice) were injected intravitreally with sulfo-SBED-labeled AXT107, and their retinas were isolated after 24h. Bound peptide was then cross-linked using UV reactive chemistry, and the tissue was lysed. Each lysate was then separated into three types of samples called input, pull-down, or flowthrough for the lysates before pull-down, components that associated with the beads, and components that did not associate with the beads, respectively.

(A–D) Input samples from each treatment set were separated by SDS-PAGE and analyzed by western blot for the levels of integrins α_5 (A), α_v (B), β_1 (C), and β_3 (D) with β-tubulin as a loading control.

(E–G) Input, pull-down, and flowthrough samples from each of the three datasets resolved by SDS-PAGE and analyzed for integrins α_5 (E), α_v (F), and β_1 and β_3 (G) with β-tubulin as a loading control. Input samples for integrin α_5 are an extended cropping of the gel used for panel A. Conversely, the input samples in panels F and G are included to allow same gel comparisons of the three different samples but were rerun for panels B, C, and D to address an overloading artifact in lane 1. Owing to differences in molecular weights and staining intensity, integrins β_1 and β_3 were stained serially on the same blot.

AXT107. The suppression of NV at longer time points after AXT107 precludes assessing the localization of AXT107 at time points beyond 3 days after injection. In normal eyes, no signal for AXT107 was detectable by either approach in association with blood vessels or elsewhere in the retina. Apparently, without sufficient levels of its integrin-binding partners, AXT107 was not retained for even 24 h in the retina in levels sufficient to visualize it. In contrast, in 3 models of retinal/choroidal vascular disease, by both techniques, AXT107 co-localized with $\alpha_v\beta_3$ and $\alpha_5\beta_1$ on abnormal vessels at 1 and 3 days after injection. These findings were also partially supported by the western blots of the inputs from the cross-linking studies. The expression of both integrins α_v and β_3 was found to increase in OIR mice relative to those reared in room air. Conversely,

increased expression was only visible in one set of OIR mice for integrin β_1 and not at all for integrin α_5. This was not completely surprising as integrins α_v, β_1, and β_3 are all reportedly upregulated during hypoxia[52] but struggles to explain the induction of integrin $\alpha_5\beta_1$ expression observed between the normal and disease-mimicking states in the *in vivo* models. As integrin α_5 is only reported to interact with integrin β_1 and its surface presentation depends on its interaction with integrin β_1,[53] the variable expression of integrin β_1 seen in the cross-linking experiments may contribute to the observed increases in integrin $\alpha_5\beta_1$ expression by stabilizing the integrin α_5 within the NV in these *in vivo* models. Moreover, hypoxia may also influence integrin $\alpha_5\beta_1$ indirectly by increasing the expression of fibronectin,[54,55] which has been shown to stabilize the levels of integrin α_5.[56]

The increased levels of $\alpha_v\beta_3$ and $\alpha_5\beta_1$ in diseased retinal/choroidal vessels compared to their normal counterparts are consistent with observations in other tissues. Integrin $\alpha_v\beta_3$ is expressed on angiogenic blood vessels in granulation tissue or within brain tumors but not blood vessels in normal skin or normal brain.[22,57] Phage that displayed a peptide that selectively binds $\alpha_v\beta_3$ homed to tumors in mice and was not detectable in several normal tissues showing the differential expression of $\alpha_v\beta_3$ on tumor vessels compared to normal vessels.[58] After cerebral infarction, angiogenesis occurs in the penumbra and $\alpha_5\beta_1$ is detectable on the new vessels but not other brain vessels.[59] This differential expression of $\alpha_v\beta_3$ and $\alpha_5\beta_1$ on endothelial cells participating in angiogenesis versus quiescent endothelial cells may have therapeutic and safety benefits because integrin $\alpha_v\beta_3$ antagonists induce apoptosis in endothelial cells of tumor vessels promoting tumor regression but have no effect on normal vessels.[23]

Hypoxia and VEGF have been shown to increase expression of $\alpha_v\beta_3$ and $\alpha_5\beta_1$ on retinal microvascular endothelial cells in culture,[60] and there is evidence that in the absence of hypoxia, VEGF stimulates upregulation of $\alpha_v\beta_3$ and $\alpha_5\beta_1$ on endothelial cells *in vivo* because immunostaining for $\alpha_v\beta_3$ and $\alpha_5\beta_1$ was absent or weak on iris vessels in monkey eyes but showed strong staining for each after four intraocular injections of 0.5 μg VEGF 9 days after the first injection.[61] Consistent with this, we observed immunostaining for $\alpha_v\beta_3$ and $\alpha_5\beta_1$ on some retinal vessels within the retina in *rho/VEGF* transgenic mice with increased expression of VEGF in photoreceptors in which there is no hypoxia. VEGF is a critical stimulus for excessive vascular leakage as well as NV.[12,43] Thus, AXT107 should target endothelial cells with VEGF-induced activation and disruption of cell-cell junctions and suppress vascular leakage, explaining the leakage-suppressing activity of AXT107 in rabbit eyes injected with VEGF.[21]

In conclusion, the current study adds to the body of evidence suggesting that AXT107 exerts its beneficial effects in models of retinal/choroidal vascular disease through binding of $\alpha_v\beta_3$ and $\alpha_5\beta_1$. These two integrins are differentially expressed on diseased versus normal retinal vessels providing a mechanism by which AXT107 is targeted to where it is needed and minimizing exposure elsewhere. By binding $\alpha_v\beta_3$, AXT107 suppresses phosphorylation and downstream signaling of VEGF receptors and hence blocks a validated target that plays a major role in stimulating the diseases. By binding $\alpha_5\beta_1$, AXT107 activates Tie2, a second clinically validated target for the diseases. Hence, AXT107 acts on two critical pathways in diseased retinal vessels and hence is a single agent yielding combination therapy providing strong rationale for its use in a variety of retinal/choroidal vascular diseases including nAMD, diabetic macular edema, and retinal vein occlusions.

Limitations of the study

This study demonstrates co-localization of AXT107 on pathologic blood vessels in animal models of retinal vascular disease in which AXT107 provides therapeutic benefits, but it doesn't provide quantitative assessment of binding. This limitation is mitigated by the prior demonstration of saturation binding with binding affinity in the nM range between each of the integrins and AXT107 *in vitro*. The absence of AXT107 localization on blood vessels with undetectable expression of $\alpha_v\beta_3$ and $\alpha_5\beta_1$ is also supportive.

STAR★METHODS

Detailed methods are provided in the online version of this paper and include the following:

- KEY RESOURCES TABLE
- RESOURCE AVAILABILITY
  - Lead contact
  - Materials availability
  - Data and code availability

SUPPLEMENTAL INFORMATION

Supplemental information can be found online at https://doi.org/10.1016/j.isci.2023.106078.

ACKNOWLEDGMENTS

Funding: This research was supported by NIH grant R01EY028996 and the Office of the Director of the National Institutes of Health under award number S10OD016374.

AUTHOR CONTRIBUTIONS

Conceptualization: RLS, ACM, JJG, ASP, NBP, and PAC.

Methodology: RLS, ACM, JJG, ASP, NBP, and PAC.

Investigation: RLS and ACM.

Visualization: RLS, ACM, SYT, JJG, ASP, NBP, and PAC.

Supervision: JJG, ASP, NBP, and PAC.

Writing—original draft: RLS and PAC;

Writing—review & editing: RLS, ACM, SYT, JJG, ASP, NBP, and PAC.

DECLARATION OF INTERESTS

Related to current manuscript:

NBP is the Vice President, R&D, and JJG is the Chief Technology Advisor and a member of the board of directors.

ASP is the Chief Scientific Advisor, and PAC is a consultant for AsclepiX Therapeutics, Inc.

NBP, ACM, JJG, and ASP hold equity in and receive income from AsclepiX.

NBP, ACM, ASP, and JJG are co-inventors on pending and awarded patents related to this work filed by Johns Hopkins University.

Unrelated to current manuscript:

PAC: Ownership: Stock Options in Graybug, Allegro, and Cove.

Research Support: Genentech, Mallinckrodt Pharmaceuticals, RegenxBio, Sanofi.

Intellectual Property: Co-inventor on unrelated pending and awarded patents.

JJG: Ownership: Stock Options in Cove and Dome.

Income: Tidal.

Research Support: AstraZeneca and GlaxoSmithKline.

Intellectual Property: Co-inventor on unrelated pending and awarded patents.

ASP: Income: CytomX Therapeutics.

Research Support: AstraZeneca, Boehringer Ingelheim, CytomX Therapeutics.

Intellectual Property: Co-inventor on unrelated pending and awarded patents.

Received: August 1, 2022
Revised: December 22, 2022
Accepted: January 23, 2023
Published: January 30, 2023

REFERENCES

1. Wong, W.L., Su, X., Li, X., Cheung, C.M.G., Klein, R., Cheng, C.Y., and Wong, T.Y. (2014). Global prevalence of age-related macular degeneration and disease burden projection for 2020 and 2040: a systematic review and meta-analysis. Lancet Global Health *2*, e106–e116. https://doi.org/10.1016/S2214-109X(13)70145-1.

2. Yau, J.W.Y., Rogers, S.L., Kawasaki, R., Lamoureux, E.L., Kowalski, J.W., Bek, T., Chen, S.J., Dekker, J.M., Fletcher, A., Grauslund, J., et al. (2012). Global prevalence and major risk factors of diabetic retinopathy. Diabetes Care *35*, 556–564. https://doi.org/10.2337/dc11-1909.

3. Mitchell, P., Liew, G., Gopinath, B., and Wong, T.Y. (2018). Age-related macular degeneration. Lancet *392*, 1147–1159. https://doi.org/10.1016/S0140-6736(18)31550-2.

4. Mullins, R.F., Johnson, M.N., Faidley, E.A., Skeie, J.M., and Huang, J. (2011). Choriocapillaris vascular dropout related to density of drusen in human eyes with early age-related macular degeneration. Invest. Ophthalmol. Vis. Sci. *52*, 1606–1612. https://doi.org/10.1167/iovs.10-6476.

5. Mullins, R.F., Schoo, D.P., Sohn, E.H., Flamme-Wiese, M.J., Workamelahu, G., Johnston, R.M., Wang, K., Tucker, B.A., and Stone, E.M. (2014). The membrane attack complex in aging human choriocapillaris. Relationship to macular degeneration and choroidal thinning. Am. J. Pathol. *184*, 3142–3153. https://doi.org/10.1016/j.ajpath.2014.07.017.

6. Shimizu, K., Kobayashi, Y., and Muraoka, K. (1981). Midperipheral fundus involvement in diabetic retinopathy. Ophthalmology *88*, 601–612. https://doi.org/10.1016/s0161-6420(81)34983-5.

7. Ozaki, H., Yu, A.Y., Della, N., Ozaki, K., Luna, J.D., Yamada, H., Hackett, S.F., Okamoto, N., Zack, D.J., Semenza, G.L., and Campochiaro, P.A. (1999). Hypoxia inducible factor-1a is increased in ischemic retina: temporal and spatial correlation with VEGF expression. Invest. Ophthalmol. Vis. Sci. *40*, 182–189.

8. Kelly, B.D., Hackett, S.F., Hirota, K., Oshima, Y., Cai, Z., Berg-Dixon, S., Rowan, A., Yan, Z., Campochiaro, P.A., and Semenza, G.L. (2003). Cell type-specific regulation of angiogenic growth factor gene expression and induction of angiogenesis in nonischemic tissue by a constitutively active form of hypoxia-inducible factor 1. Circ. Res. *93*, 1074–1081. https://doi.org/10.1161/01.RES.0000102937.50486.

9. Yoshida, T., Zhang, H., Iwase, T., Shen, J., Semenza, G.L., and Campochiaro, P.A. (2010). Digoxin inhibits retinal ischemia-induced HIF-1alpha expression and ocular neovascularization. Faseb. J. *24*, 1759–1767. https://doi.org/10.1096/fj.09-145664.

10. Iwase, T., Fu, J., Yoshida, T., Muramatsu, D., Miki, A., Hashida, N., Lu, L., Oveson, B., Lima e Silva, R., Seidel, C., et al. (2013). Sustained delivery of a HIF-1 antagonist for ocular neovascularization. J. Contr. Release *172*, 625–633.

11. Zeng, M., Shen, J., Liu, Y., Lu, L.Y., Ding, K., Fortmann, S.D., Khan, M., Wang, J., Hackett, S.F., Semenza, G.L., and Campochiaro, P.A. (2017). The HIF-1 antagonist acriflavine: visualization in retina and suppression of ocular neovascularization. J. Mol. Med. *95*, 417–429. https://doi.org/10.1016/j.jconrel.2013.10.008.

12. Campochiaro, P.A., Aiello, L.P., and Rosenfeld, P.J. (2016). Anti-vascular endothelial growth factor agents in the treatment of retinal disease. From bench to bedside. Ophthalmology *123*, S78–S88. https://doi.org/10.1016/j.ophtha.2016.04.056.

13. Hackett, S.F., Ozaki, H., Strauss, R.W., Wahlin, K., Suri, C., Maisonpierre, P., Yancopoulos, G., and Campochiaro, P.A. (2000). Angiopoietin 2 expression in the retina: upregulation during physiologic and pathologic neovascularization. J. Cell. Physiol. *184*, 275–284. https://doi.org/10.1002/1097-4652(275)184:3<275::AID-JCP1>3.0.CO;2-7.

14. Hackett, S.F., Wiegand, S., Yancopoulos, G., and Campochiaro, P.A. (2002). Angiopoietin-2 plays an important role in retinal angiogenesis. J. Cell. Physiol. *192*, 182–187. https://doi.org/10.1002/jcp.10128.

15. Gale, N.W., Thurston, G., Hackett, S.F., Renard, R., Wang, Q., McClain, J., Martin, C., Witte, C., Witte, M.H., Jackson, D., et al. (2002). Angiopoietin-2 is required for postnatal angiogenesis and lymphatic patterning, and only the latter role is rescued by angiopoietin-1. Dev. Cell *3*, 411–423. https://doi.org/10.1016/s1534-5807(02)00217-4.

16. Sahni, J., Patel, S.S., Dugel, P.U., Khanani, A.M., Jhaveri, C.D., Wykoff, C.C., Hershberger, V.S., Pauly-Evers, M., Sadikhov, S., Szczesny, P., et al. (2019). Simultaneous inhibition of angiopoietin-2 and vascular endothelial growth factor-A with faricimab in diabetic macular edema: BOULEVARD phase 2 randomized trial. Ophthalmology *126*, 1155–1170. https://doi.org/10.1016/j.ophtha.2019.03.023.

17. Sahni, J., Dugel, P.U., Patel, S.S., Chittum, M.E., Berger, B., Del Valle Rubido, M., Sadikhov, S., Szczesny, P., Schwab, D., Nogoceke, E., et al. (2020). Safety and efficacy of different doses and regimens of faricimab vs ranibizumab in neovascular age-related macular degeneration; the AVENUE phase 2 randomized clinical trial. JAMA Ophthalmol. *138*, 955–963. https://doi.org/10.1001/jamaophthalmol.2020.2685.

18. Khanani, A.M., Skelly, A., Bezlyak, V., Griner, R., Torres, L.R., and Sagkriotis, A. (2020). SIERRA-AMD: a retrospective, real-world evidence study of patients with neovascular age-related macular degeneration in the United States. Ophthalmol. Retina *4*, 122–133. https://doi.org/10.1016/j.oret.2019.09.009.

19. Karagiannis, E.D., and Popel, A.S. (2008). A systematic methodology for proteome-wide identification of peptides inhibiting the proliferation and migration of endothelial cells. Proc. Natl. Acad. Sci. USA *105*, 13775–13780. https://doi.org/10.1073/pnas.0803241105.

20. Rosca, E.V., Koskimaki, J.E., Pandey, N.B., Tamiz, A.P., and Popel, A.S. (2012). Structure-activity relationship of collagen derived anti-angiogenic biomimetic peptides. Chem. Biol. Drug Des. *80*, 27–37. https://doi.org/10.1111/j.1747-0285.2012.01376.x.

21. Lima e Silva, R., Kanan, Y., Mirando, A.C., Kim, J., Shmueli, R.B., Lorenc, V.E., Fortmann, S.D., Sciamanna, J., Pandey, N.B., Green, J.J., et al. (2017). Tyrosine kinase blocking collagen IV-derived peptide suppresses ocular neovascularization and vascular leakage. Sci. Transl. Med. *9*, eaai8030. https://doi.org/10.1126/scitranslmed.aai8030.

22. Brooks, P.C., Clark, R.A., and Cheresh, D.A. (1994). Requirement of vascular integrin alpha-v beta-3 for angiogenesis. Science *264*, 569–571. https://doi.org/10.1126/science.7512751.

23. Brooks, P.C., Montgomery, A.M., Rosenfeld, M., Reisfeld, R.A., Hu, T., Klier, G., and Cheresh, D.A. (1994). Integrin alpha v beta 3 antagonists promote tumor regression by inducing apoptosis of angiogenic blood vessels. Cell *79*, 1157–1164. https://doi.org/10.1016/0092-8674(94)90007-8.

24. Friedlander, M., Theesfeld, C.L., Sugita, M., Fruttiger, M., Thomas, M.A., Chang, S., and Cheresh, D.A. (1996). Involvement of integrins alpha-v beta-3 and alpha-v beta-5 in ocular neovascular diseases. Proc. Natl. Acad. Sci. USA *93*, 9764–9769. https://doi.org/10.1073/pnas.93.18.9764.

25. Kim, S., Bell, K., Mousa, S.A., and Varner, J.A. (2000). Regulation of angiogenesis in vivo by ligation of integrin alpha5beta1 with the central cell-binding domain of fibronectin. Am. J. Pathol. *156*, 1345–1362. https://doi.org/10.1016/s0002-9440(10)65005-5.

26. Umeda, N., Kachi, S., Akiyama, H., Zahn, G., Vossmeyer, D., Stragies, R., and Campochiaro, P.A. (2006). Suppression and regression of choroidal neovascularization by systemic administration of an Alpha5Beta1 integrin antagonist. Mol. Pharmacol. *69*, 1820–1828. https://doi.org/10.1124/mol.105.020941.

27. Soldi, R., Mitola, S., Strasly, S., Defilippi, P., Tarone, G., and Bussolino, F. (1999). Role of avb3 integrin in the activation of vascular ednothelial growth factor receptor-2. EMBO J. *18*, 734–740. https://doi.org/10.1093/emboj/18.4.882.

28. Borges, E., Jan, Y., and Ruoslahti, E. (2000). PDGF-receptor and VEGF-receptor-2 bind to the β_3 integrin through its extracellular domain. J. Biol. Chem. *275*, 39867–39873. https://doi.org/10.1074/jbc.M007040200.

29. Mahabeleshwar, G.H., Feng, W., Reddy, K., Plow, E.F., and Byzova, T.V. (2007). Mechanisms of integrin-vascular endothelial growth factor receptor cross-activation in angiogenesis. Circ. Res. *101*, 570–580. https://doi.org/10.1161/CIRCRESAHA.107.155655.

30. Cascone, I., Napione, L., Maniero, F., Serini, G., and Bussolino, F. (2005). Stable interaction between $\alpha_5\beta_1$ integrin and Tie2 tyrosine kinase receptor regulates endothelial cell response to Ang-1. J. Cell Biol. *170*, 993–1004. https://doi.org/10.1083/jcb.200507082.

31. Dalton, A.C., Shlamkovitch, T., Papo, N., and Barton, W.A. (2016). Constitutive association of Tie1 and Tie2 with endothelial integrins is functionally modulated by angiopoietin-1 and fibronectin. PLoS One *11*, e0163732. https://doi.org/10.1371/journal.pone.0163732.

32. Mirando, A.C., Shen, J., Silva, R.L.E., Chu, Z., Sass, N.C., Lorenc, V.E., Green, J.J., Campochiaro, P.A., Popel, A.S., and Pandey, N.B. (2019). A collagen IV-derived peptide disrupts α5β1 integrin and potentiates Ang2/Tie2 signaling. JCI insight *4*, e122043. https://doi.org/10.1172/jci.insight.122043.

33. Nambu, H., Nambu, R., Oshima, Y., Hackett, S.F., Okoye, G., Wiegand, S., Yancopoulos, G., Zack, D.J., and Campochiaro, P.A. (2004). Angiopoietin 1 inhibits ocular neovascularization and breakdown of the blood-retinal barrier. Gene Ther. *11*, 865–873. https://doi.org/10.1038/sj.gt.3302230.

34. Nambu, H., Umeda, N., Kachi, S., Oshima, Y., Akiyama, H., Nambu, R., and Campochiaro, P.A. (2005). Angiopoietin 1 prevents retinal detachment in an aggressive model of proliferative retinopathy, but has no effect on established neovascularization. J. Cell. Physiol. *204*, 227–235. https://doi.org/10.1002/jcp.20292.

35. Shen, J., Frye, M., Lee, B.L., Reinardy, J.L., McClung, J.M., Ding, K., Kojima, M., Xia, H., Seidel, C., Lima e Silva, R., et al. (2014). Targeting VE-PTP activates TIE2 and stabilizes the ocular vasculature. J. Clin. Invest. *124*, 4564–4576. https://doi.org/10.1172/JCI74527.

36. Smith, L.E.H., Wesolowski, E., McLellan, A., Kostyk, S.K., D'Amato, R., Sullivan, R., and D'Amore, P.A. (1994). Oxygen-induced retinopathy in the mouse. Invest. Ophthalmol. Vis. Sci. *35*, 101–111.

37. Okamoto, N., Tobe, T., Hackett, S.F., Ozaki, H., Vinores, M.A., LaRochelle, W., Zack, D.J., and Campochiaro, P.A. (1997). Transgenic mice with increased expression of vascular endothelial growth factor in the retina: a new model of intraretinal and subretinal neovascularization. Am. J. Pathol. *151*, 281–291.

38. Tobe, T., Okamoto, N., Vinores, M.A., Derevjanik, N.L., Vinores, S.A., Zack, D.J., and Campochiaro, P.A. (1998). Evolution of neovascularization in mice with overexpression of vascular endothelial growth factor in photoreceptors. Invest. Ophthalmol. Vis. Sci. *39*, 180–188.

39. Yannuzzi, L.A., Negrão, S., Iida, T., Carvalho, C., Rodriguez-Coleman, H., Slakter, J., Freund, K.B., Sorenson, J., Orlock, D., and Borodoker, N. (2001). Retinal angiomatous proliferation in age-related macular degeneration. Retina *21*, 416–434. https://doi.org/10.1097/00006982-200110000-00003.

40. Tobe, T., Ortega, S., Luna, J.D., Ozaki, H., Okamoto, N., Derevjanik, N.L., Vinores, S.A., Basilico, C., and Campochiaro, P.A. (1998). Targeted disruption of the *FGF2* gene does not prevent choroidal neovascularization in a murine model. Am. J. Pathol. *153*, 1641–1646. https://doi.org/10.1016/S0002-9440(10)65753-7.

41. Rosca, E.V., Penet, M.F., Mori, N., Koskimaki, J.E., Lee, E., Pandey, N.B., Bhujwalla, Z.M., and Popel, A.S. (2014). A biomimetic collagen derivived peptide exhibits anti-angiogenic activity in triple negative breast cancer. PLoS One *9*, e111901. https://doi.org/10.1371/journal.pone.0111901.

42. Aiello, L.P., Pierce, E.A., Foley, E.D., Takagi, H., Chen, H., Riddle, L., Ferrara, N., King, G.L., and Smith, L.E. (1995). Suppression of retinal neovascularization in vivo by inhibition of vascular endothelial growth factor (VEGF) using soluble VEGF-receptor chimeric proteins. Proc. Natl. Acad. Sci. USA *92*, 10457–10461. https://doi.org/10.1073/pnas.92.23.10457.

43. Ozaki, H., Hayashi, H., Vinores, S.A., Moromizato, Y., Campochiaro, P.A., and Oshima, K. (1997). Intravitreal sustained release of VEGF causes retinal neovascularization in rabbits and breakdown of the blood-retinal barrier in rabbits and primates. Exp. Eye Res. *64*, 505–517. https://doi.org/10.1006/exer.1996.0239.

44. Seo, M.-S., Kwak, N., Ozaki, H., Yamada, H., Okamoto, N., Yamada, E., Fabbro, D., Hofmann, F., Wood, J.M., and Campochiaro, P.A. (1999). Dramatic inhibition of retinal and choroidal neovascularization by oral administration of a kinase inhibitor. Am. J. Pathol. *154*, 1743–1753. https://doi.org/10.1016/S0002-9440(10)65430-2.

45. Kwak, N., Okamoto, N., Wood, J.M., and Campochiaro, P.A. (2000). VEGF is an important stimulator in a model of choroidal neovascularization. Invest. Ophthalmol. Vis. Sci. *41*, 3158–3164.

46. Rosenfeld, P.J., Brown, D.M., Heier, J.S., Boyer, D.S., Kaiser, P.K., Chung, C.Y., and Kim, R.Y.; MARINA Study Group (2006). Ranibizumab for neovascular age-related macular degeneration. N. Engl. J. Med. *355*, 1419–1431. https://doi.org/10.1056/NEJMoa05448147.

47. Brown, D.M., Kaiser, P.K., Michels, M., Soubrane, G., Heier, J.S., Kim, R.Y., Sy, J.P., and Schneider, S.; ANCHOR Study Group (2006). Ranibizumab versus verteporfin for neovascular age-related macular degeneration. N. Engl. J. Med. *355*, 1432–1444. https://doi.org/10.1056/NEJMoa062655.

48. Mirando, A.C., Lima e Silva, R., Chu, Z., Campochiaro, P.A., Pandey, N.B., and Popel, A.S. (2020). Suppression of ocular vascular inflammation through peptide-mediated activation of angiopoietin-Tie2 signaling. Int. J. Mol. Sci. *21*, 5142. https://doi.org/10.3390/ijms21145142.

49. Campochiaro, P.A., Khanani, A., Singer, M., Patel, S., Boyer, D., Dugel, P., Kherani, S., Withers, B., Gambino, L., Peters, K., et al. (2016). Enhanced benefit in diabetic macular edema from AKB-9778 Tie2 activation combined with vascular endothelial growth factor suppression. Ophthalmology *123*, 1722–1730. https://doi.org/10.1016/j.ophtha.2016.04.025.

50. Heier, J.S., Khanani, A.M., Quezada Ruiz, C., Basu, K., Ferrone, P.J., Brittain, C., Figueroa, M.S., Lin, H., Holz, F.G., Patel, V., et al. (2022). Efficacy, durability, safety of intravitreal faricimab up to every 16 weeks for neovascular age-related macular degeneration (TENAYA and LUCERNE): two randomised, double-masked, phase 3, non-inferiority trials. Lancet *399*, 729–740. https://doi.org/10.1016/S0140-6736(22)00010-1.

51. Wykoff, C.C., Abreu, F., Adamis, A.P., Basu, K., Eichenbaum, D.A., Haskova, Z., Lin, H., Loewenstein, A., Mohan, S., Pearce, I.A., et al. (2022). Efficacy, durability, and safety of intravitreal faricimab with extended dosing up to every 16 weeks in patients with diabetic macular oedema (YOSEMITE and RHINE): two randomized, double-masked, phase 3 trials. Lancet *399*, 741–755. https://doi.org/10.1016/S0140-6736(22)00018-6.

52. Befani, C., and Liakos, P. (2017). Hypoxia upregulates integrin gene expression in microvascular endothelial cells and promotes their migration and capillary-like tube formation. Cell Biol. Int. *41*, 769–778. https://doi.org/10.1002/cbin.10777.53.

53. Huet-Calderwood, C., Rivera-Molina, F., Iwamoto, D.V., Kromann, E.B., Toomre, D., and Calderwood, D.A. (2017). Novel ecto-tagged integrins reveal their trafficking in live cells. Nat. Commun. *8*, 570. https://doi.org/10.1038/s41467-017-00646-w.

54. Lee, S.H., Lee, Y.J., and Han, H.J. (2011). Role of hypoxia-induced fibronectin-integrin β1 expression in embryonic stem cell proliferation and migration: involvement of PI3K/Akt and FAK. J. Cell. Physiol. *226*, 484–493. https://doi.org/10.1002/jcp.22358.

55. Milner, R., Hung, S., Erokwu, B., Dore-Duffy, P., LaManna, J.C., and del Zoppo, G.J. (2008). Increased expression of fibronectin and the alpha 5 beta 1 integrin in angiogenic cerebral blood vessels of mice subject to hypobaric hypoxia. Mol. Cell. Neurosci. *38*, 43–52. https://doi.org/10.1016/j.mcn.2008.01.013.

56. Hsia, H.C., Nair, M.R., and Corbett, S.A. (2014). The fate of internalized α5 integrin is regulated by matrix-capable fibronectin. J. Surg. Res. *191*, 268–279. https://doi.org/10.1016/j.jss.2014.05.084.

57. Bello, L., Francolini, M., Marthyn, P., Zhang, J., Carroll, R.S., Nikas, D.C., Strasser, J.F., Villani, R., Cheresh, D.A., and Black, P.M. (2001). avb3 and avb5 integrin expression in glioma periphery. Neurosurgery *49*, 380–389. https://doi.org/10.1097/00006123-200108000-00022.

58. Pasqualini, R., Koivunen, E., and Ruoslahti, E. (1997). Alpha v integrins as receptors for tumor targeting by circulating ligands. Nat. Biotechnol. *15*, 542–546. https://doi.org/10.1038/nbt0697-542.

59. Sun, J., Yu, L., Huang, S., Lai, X., Milner, R., and Li, L. (2017). Vascular expression of angiopoietin 1, a5B1 integrin and tight junction proteins is tightly regulated during vascular remodeling in the post-ischemic brain. Neuroscience *362*, 248–256. https://doi.org/10.1016/j.neuroscience.2017.08.040.

60. Suzuma, K., Takagi, H., Otani, A., and Honda, Y. (1998). Hypoxia and vascular endothelial growth factor stimulate angiogenic integrin expression in bovine retinal microvascular endothelial cells. Invest. Ophthalmol. Vis. Sci. *39*, 1028–1035.

61. Witmer, A.N., van Blijswijk, B.C., van Noorden, C.J.F., Vrensen, G.F.J.M., and Schlingemann, R.O. (2004). In vivo angiogenic phenotype of endothelial cells and pericytes induced by vascular endothelial growth factor. J. Histochem. Cytochem. *52*, 39–52. https://doi.org/10.1177/002215540405200105.

62. Tsujinaka, H., Fu, J., Shen, J., Yu, Y., Hafiz, Z., Kays, J., McKenzie, D., Cardona, D., Culp, D., Peterson, W., et al. (2020). Sustained treatment of retinal vascular diseases with self-aggregating sunitinib microparticles. Nat. Commun. *11*, 694. https://doi.org/10.1038/s41467-020-14340-x.

63. Saishin, Y., Saishin, Y., Takahashi, K., Lima e Silva, R., Hylton, D., Rudge, J.S., Wiegand, S.J., and Campochiaro, P.A. (2003). VEGF-TRAP$_{R1R2}$ suppresses choroidal neovascularization and VEGF-induced breakdown of the blood-retinal barrier. J. Cell. Physiol. *195*, 241–248. https://doi.org/10.1002/jcp.10246.

STAR★METHODS

KEY RESOURCES TABLE

REAGENT or RESOURCE	SOURCE	IDENTIFIER
Antibodies		
Polyclonal rabbit anti-AXT107	Covance Immunology Services	PR191108B
HRP-conjugated goat anti-rabbit IgG	Cell Signaling Technologies	Cat # 7074; RRID:AB_2099233
Integrin Alpha-V Beta-3 Antibody	Abbiotec	Cat# 251672; RRID:AB_10643501
Integrin Alpha-5 Beta-1 Antibody	Novus Biological	Cat # nbp2-29788
Anti-Integrin alpha5, C-terminus, intracellular antibody	Millipore Sigma	Cat# AB1928; RRID:AB_2128185
Anti-Integrin alphaV, C-terminus, Intracellular antibody	Millipore Sigma	Cat# AB1930; RRID:AB_390210
Alexa Fluor 488-conjugated donkey anti-rabbit IgG	Thermo Fisher Scientific	Cat# R37118; RRID:AB_2556546
Alexa Fluor 488-conjugated donkey anti-rat IgG	Thermo Fisher Scientific	Cat# A-21208; RRID:AB_2535794
DyLight 594-conjugated donkey anti-rabbit IgG	Thermo Fisher Scientific	Cat# SA5-10040; RRID:AB_2556620
Goat Anti-Mouse IgG Alexa Fluor 594	Abcam	Cat# ab150116; RRID:AB_2650601
Normal Rabbit IgG antibody	Millipore Sigma	Cat# NI01-100UG; RRID:AB_490574
Normal rat IgG	Millipore Sigma	Cat# NI04
Alexa Fluor 488-conjugated goat anti-rabbit	Thermo Fisher Scientific	Cat# A-11034; RRID:AB_2576217
Alexa Fluor 594-conjugated goat anti-rabbit IgG	Thermo Fisher Scientific	Cat# A32740; RRID:AB_2762824
Alexa Fluor 594-conjugated goat anti-mouse IgG	Thermo Fisher Scientific	Cat# A32742; RRID:AB_2762825
Chemicals, peptides, and recombinant proteins		
Complete Protease Inhibitor Cocktail	Sigma	Cat# CO-RO
Xylazine hydrochloride	Covetrus	SKU 061035
Ketamine hydrochloride	Covetrus	SKU 071069
Paraformaldehyde aqueous solution 32%	Electron Microscopy Section	Cat# 15714
Optimal Cutting Temperature (O.C.T.)	Tissue Tek	Cat# 4583
Tropicamide Ophthalmic solutions	Alcon Labs, Inc.	Cat# 61314–35502
AXT107 peptide	Vivitide	Lot#: LP02395-2
FAM-AXT107	GenScript	Lot#: U086FGA110-1/PE3038
SP2048	Vivitide	Lot#: A7118-4
SDS-loading buffer	Cell Signaling Technologies	Cat#: 56036
BSA	Cell Signaling Technologies	Cat#: 9998
Tween 20, Molecular Biology Grade	Promega	Cat#: H5151
Super-Signal West Pico PLUS	Thermo Fisher Scientific	Cat # PI34580
Normal goat serum	Vector	Cat # S-1000; RRID:AB_2336615
FITC-conjugated Griffonia Simplicifolia agglutinin lectin	Vector	Cat # FL-1101; RRID:AB_2336490
Lectin GS-II From *Griffonia simplicifolia*, Alexa Fluor™ 594 Conjugate	Thermo Fisher Scientific	Cat #L21416

(*Continued on next page*)

Continued

REAGENT or RESOURCE	SOURCE	IDENTIFIER
Hoechst 33342	Thermo Fisher Scientific	Cat #H3570
Aqueous Mounting AquaPoly solution	Neobits	Cat # 18606–5
Normal goat serum	Thermo Fisher Scientific	Cat# 31872, RRID:AB_2532166
Sulfo-SBED Biotin Label Transfer Reagent	Thermo Fisher Scientific	Cat# 33033
Streptavidin (Sepharose Bead Conjugate)	Cell Signaling Technologies	Cat#: 3419
Experimental models: Cell lines		
Human umbilical vein endothelial cells	Lifeline Cell Technology	FC-0044
VascuLife VEGF Endothelial Medium	Lifeline Cell Technology	LL-0003
Experimental models: Organisms/strains		
Mouse: C57BL/6J	The Jackson Laboratories	RRID:IMSRJAX:000664
Mouse: *rho*/VEGF transgenic mice	The Campochiaro Laboratory	B6-Tg (bRhdopsin-hVEGF-165) 6Pac
Software and algorithms		
SPOT RT 4.6 software	Diagnostic Instruments Inc.	http://www.spotimaging.com/software/spot-advanced/; RRID:SCR_016613
ImageJ software	NIH	http://rsb.info.nih.gov/nih-image/index.html
Infinity Capture v. 6.5.6 software	Teledyne Lumenera	https://infinity-software1.software.informer.com/6.5/
Other		
OcuLight GL Photocoagulator	Iridex	33003 EN
Harvard Pump Microinjection System	Harvard Appparatus	Cat# 65–0001
Borosilicate Glass Capillaries	World Precision Instruments	Cat# TW100-4
iBright FL1000 imager	Invitrogen	N/A
Zeiss Axioskop 2 Plus	Carl Zeiss	N/A
Zeiss AxioObserver; LSM700 confocal module	Carl Zeiss	N/A
Olympus IX71	Olympus Life Science	N/A
CL-1000 UV Crosslinker	Analytik Jena	N/A

RESOURCE AVAILABILITY

Lead contact

Further information and requests for resources and reagents should be directed to and will be fulfilled by the lead contact, Peter A. Campochiaro (pcampo@jhmi.edu).

Materials availability

This study did not generate new unique reagents. Transgenic mice used in the study will be provided upon request.

All data needed to evaluate the manuscript are available in the figures and supplemental figures.

No code was generated in this study.

Any additional information required to reanalyze the data reported in this paper is available from the lead contact upon request.

Data and code availability

All data needed to evaluate the conclusions in the paper are present in the paper and/or the supplemental information. No new code was generated in this study.

EXPERIMENTAL MODELS AND SUBJECT DETAILS

All wild-type C57BL/6J mice were purchased by The Jackson Laboratories (Bar Harbor, ME) while the *rho*/VEGF transgenic mice were bred in our animal facility. All the mice were housed in a specific pathogen free environment at our animal facility at Johns Hopkins University with free access to food and water. All animals used in our research are covered by the Animal Care and Use Program which follows the Animal Welfare Act regulations and Public Health Service Policy. Mice were treated in accordance with the Association for Research in Vision and Ophthalmology Guidelines regarding the care and use of animals in research. All procedures and experiments were approved by the IACUC of Johns Hopkins University. There are no data to suggest that sex has any effect on outcomes tested in all the models that were used and therefore mice of both sexes were used in all experiments in roughly equal numbers. A minimum of 20 ocular sections were assessed per group and all experiments were done in duplicates. Qualitatively similar results were found in each replicate.

METHOD DETAILS

Mice with OIR

The OIR mouse model is a widely used model of ischemia-induced retinal NV.[21,32,36,62] At postnatal day 7 (P7) C57BL/6 mice and their mothers were placed in an airtight incubator and exposed to 75 $\pm$ 3% oxygen for 5 days. They were returned to room air at P12. At P17, mice were euthanized with xylazine hydrochloride (10 mg/kg, Covetrus, Dublin, OH) and ketamine hydrochloride (50 mg/kg, Covetrus, Dublin, OH), eyes were fixed in paraformaldehyde 4% (Electron Microscopy Section, Hatfield, PA) for 10 min and frozen in optimal cutting temperature medium (OCT, Tissue Tek, Torrance, CA) for ocular sections or retinas were dissected for retinal flat mounts. OIR mice and age-matched room air control animals were immunostained with integrins α_v (n = 10), α_5 (n = 10), $\alpha_v\beta_3$ (n = 10) or $\alpha_5\beta_1$ (n = 10). Some mice with OIR received a 1 μL intraocular injection containing 1 μg of AXT107, or PBS at P16 and after 24 h they were euthanized and the eyes were fixed as described above (n = 20 mice). Another group of mice received 1 μL intraocular injection containing 1 μg of FAM-AXT107 or PBS at P14 (n = 10) or at P16 (n = 10). Eyes were collected at P17 for ocular sections and immunohistochemistry. A third group received intraocular injections of 1 μL containing 1 μg of sulfo-SBED labeled-AXT107 (n = 7) or PBS (n = 7) were given at P16 and 24 h later mice were euthanized, and the eyes were put in PBS for crosslinking studies (see sulfo-SBED crosslinking below).

Mice with choroidal NV due to laser-induced rupture of Bruch's membrane

Adult C57BL/6 mice with laser-induced rupture of Bruch's membrane develop type 2 choroidal NV that grows from the choroid into the subretinal space and is the predominant type of NV seen in patients with nAMD.[40,63] Five-six-week-old C57BL/6J mice were anesthetized with xylazine hydrochloride (10 mg/kg) and ketamine hydrochloride (50 mg/kg) and the pupils were dilated with 1% tropicamide (Akorn Labs, Inc., Lake Forrest, IL). Three burns of 532 nm diode laser photocoagulation (75 μm spot size, 0.1 s duration, 120 mW) were delivered to each retina using the slit lamp delivery system of an OcuLight TX GL Photocoagulator (Iridex, Mountain View, CA) and a hand-held cover slide as a contact lens. Burns were performed in the 9, 12 and 3 o'clock positions of the posterior pole of the retina. Production of a bubble at the time of laser, which indicates rupture of Bruch's membrane, is an important factor in obtaining CNV, so only burns in which a bubble was produced were included in the study. Six days after laser, 20 mice received intravitreous injections of 1 μL containing 1 μg of AXT107 or PBS under a dissecting microscope with a Harvard Pump Microinjection System (Harvard Appparatus, Inc., Holliston, MA) and pulled glass micropipettes (World Precision Instruments, Sarasota, FL). Seven days after rupture of Bruch's membrane, mice were euthanized and eyes were fixed as described above. After fixation, the anterior segment was removed, retinas were dissected and removed and eyecups containing the RPE, choroid, and sclera were used for immunofluorescent staining.

Transgenic mice with VEGF-induced NV

Transgenic mice in which the rhodopsin promoter drives expression of $VEGF_{165}$ in photoreceptors develop NV that sprouts from the deep capillary bed of the retina, grows into the subretinal space, and is extensive by P21.[37,38] At P20, *rho/VEGF* mice and littermate age-matched control (n = 10) were chosen randomly and given a 1 μL intraocular injection containing 1 μg of AXT107 (n = 10), 1 μg of FAM-AXT107 (n = 10), or PBS (n = 10) in the fellow eye. The mice were euthanized at P21 and eyes were fixed as described above. Some eyes were frozen in OCT embedding media for frozen ocular sections (n = 40) and others had the anterior segment removed and the retina dissected and removed for retinal flat mounts (n = 40). Some *rho*/VEGF

mice received 1 μL intraocular injection containing 1 μg of FAM-AXT107 or PBS at P18 (n = 10). Eyes were collected and fixed at P21 for ocular sections and immunohistochemistry.

Reagents and cells

The structure and characteristics of AXT107 have been previously described.[21] For the current study, AXT107 and SP2048 were manufactured by solid-state synthesis at Vivitide (Gardner, MA) and amidated on the C-terminal end. AXT107 was labeled on the N-terminus with 5-carboxyfluorescein (FAM-AXT107) and amidated on the C-terminus by GenScript (Piscataway, NJ). Polyclonal rabbit anti-AXT107 antibodies were prepared and purified by Covance Immunology Services (Princeton, NJ). Human umbilical vein endothelial cells (HUVECs) and endothelial growth medium, VascuLife VEGF Endothelial Medium, were purchased from Lifeline Cell Technology (Frederick, MD). Human umbilical vein endothelial cells (HUVECs) stocks were purchased from Lifeline Cell Technology (Frederick, MD) as a ten-donor pool of unspecified sex, to reduce the effects of individual variability on results, and certified to be free of contamination, including mycoplasma. These cells were cultured in VascuLife VEGF Endothelial Medium (Lifeline Cell Technology, Frederick, MD) in a humidified incubator at 37 °C and 5% CO_2.

Dot blot analysis

AXT107 or SP2048 were serially diluted in water, Blue Loading Buffer (Cell Signaling Technologies, Danvers, MA; Cat#: 56036), or HUVECs lysed in SDS-loading buffer to obtain samples and 2 μL of the resulting samples were spotted directly onto nitrocellulose membranes to obtain the amounts indicated in figure legends. The membranes were blocked with 5% BSA (Thermo Fisher Scientific, Waltham, MA) and 5% milk in tris-buffered saline containing 0.1% Tween 20 (TBST, Promega, Madison, WI) for 1 h at room temperature followed by an overnight incubation at 4°C with rabbit anti-AXT107 antibody diluted 1:500 in 5% BSA, 0.05% sodium azide in TBST. The following day, the membranes were incubated for 1 h at room temperature with HRP-conjugated goat anti-rabbit IgG (Cell Signaling Technologies, Danvers, MA; Cat # 7074) diluted 1:1000 in 5% milk in TBST. AXT107 spots were detected by chemiluminescence using Super-Signal West Pico PLUS (Thermo Fisher Scientific, Waltham, MA; Cat # PI34580) and the iBright FL1000 imager (Invitrogen, Waltham, MA).

Immunofluorescent staining

Whole eyes were frozen in optimal cutting temperature embedding media and 10 μm ocular serial sections were cut through the entire eye. Ocular sections were dried for 10 min at room temperature. After washing three times with PBS-Tween 0.2% for 15 min, the slides were blocked for 1 h at room temperature with 5% normal donkey serum (Vector, Burlingame, CA; Cat # S-1000-20). Ocular sections were incubated at 4°C overnight with rabbit antibodies directed against $\alpha_v\beta_3$ (1:100, Abbiotec, Escondido, CA; Cat # 251672), $\alpha_5\beta_1$ (1:100, Novus Biological, Centennial, CO; Cat # nbp2-29788), α_5 (1:200, Millipore Sigma, Burlington, MA; Cat # AB1928), α_v (1:200, Millipore Sigma, Burlington, MA; Cat # AB1930) or AXT107 (1:100, Asclepix, Baltimore, MD) in blocking solution. After washing, the sections were incubated with Alexa Fluor 488-conjugated donkey anti-rabbit IgG (1:400, Thermo Fisher Scientific, Waltham, MA; Cat #R37118), Alexa Fluor 488-conjugated donkey anti-rat IgG (1:400, Thermo Fisher Scientific, Waltham, MA; Cat # A21208), DyLight 594-conjugated donkey anti-rabbit IgG (1:500, Thermo Fisher Scientific, Waltham, MA; Cat # SA5-10040), Normal rabbit IgG (1:200, Millipore Sigma, Burlington, MA; Cat # NI01), Normal rat IgG (1:200, Millipore Sigma, Burlington, MA; Cat # NI04). Some sections were also incubated with FITC-conjugated *Griffonia Simplicifolia* agglutinin (GSA) lectin (1:100, Vector, Burlingame, CA; Cat # FL-1101-2) or Alexa Fluor 594-conjugated GSA lectin (1:400, Thermo Fisher Scientific, Waltham, MA; Cat #L21416) for overnight to label retinal vessels. After washing, Hoechst 33,342 (Thermo Fisher Scientific, Waltham, MA; Cat #H3570) was applied for 3 min to stain cell nuclei and sections were mounted on slides with Aqueous Mounting AquaPoly solution (Neobits, Santa Clara, CA; Cat # 18606–5) and viewed with a fluorescence microscope (Nikon Instruments Inc, New York, NY) using SPOT RT 3.4 software.

Retinas were dissected from eyes of mice with OIR or *rho*/VEGF transgenic mice and immunofluorescently stained as described above for sections, and flat mounted. Retinas from eyes of mice with choroidal NV due to laser-induced rupture of Bruch's membrane were dissected and the remaining eyecups containing RPE and choroid were immunofluorescently stained and flat mounted.

Immunofluorescent staining was also performed on cultured vascular endothelial cells using primary antibodies directed against integrin α_5 (Millipore, Burlington, MA; Cat # AB1928) or integrin α_v (Millipore, Burlington, MA; Cat # AB1930). Secondary antibodies were Alexa Fluor 488-conjugated goat anti-rabbit

(Thermo Fisher Scientific, Waltham, MA; Cat # A11034) or Alexa Fluor 594-conjugated goat anti-rabbit IgG (Thermo Fisher Scientific, Waltham, MA; Cat # A32740) or Alexa Fluor 594-conjugated goat anti-mouse IgG (Thermo Fisher Scientific, Waltham, MA; Cat # A32742). HUVECs were seeded in endothelial growth media at 1 × 10^4 cells per well in black, clear bottom, 96-well plates that were pre-coated with 10 μg/mL fibronectin. The cells were incubated in a humidified chamber at 37°C/5% CO_2 for 48 h. Media were removed, cells were washed twice with Dulbecco's PBS with calcium and magnesium (dPBS) to remove dead cells, and 100 μL of fresh growth media containing either 25 μM AXT107 (20% FAM-AXT107 and 80% unlabeled AXT107) and 5% sucrose vehicle or an equivalent volume of sucrose vehicle for control wells. After a 1.5-h incubation at 37°C, the cells were washed twice with dPBS and fixed in 3.7% paraformaldehyde for 15 min. Cells were then washed twice with dPBS and incubated in blocking buffer (5% normal goat serum, 5% chicken serum, 0.3% Triton X-100 in PBS) for 1 h at room temperature. Blocking buffer was removed and the samples were incubated in primary antibodies diluted 1:250 in dilution buffer (1% BSA in TBST) for 16 h at 4°C. Cells were washed three times with dPBS and incubated with secondary antibodies diluted 1:400 in dilution buffer for 1 h, washed twice with dPBS, and incubated in 2 μg/mL DAPI in PBS for 10 min. After two dPBS washes, cells were examined and imaged with an Olympus IX71 (Olympus Life Science, Bartlett, TN) and Infinity Capture v. 6.5.6 software. Analysis of immunohistochemistry studies were performed by a masked observer and all experiments were done in duplicates and in some cases triplicates.

Preparation of sulfo-SBED labeled peptides

For labeling AXT107, the sulfo-SBED reagent and AXT107 were dissolved in water and combined at a ratio of 3 to 1 (3 mM and 1 mM respectively). The reaction was then allowed to proceed for 4 h in the dark at room temperature. Once complete, the reaction was quenched with excess Tris-HCl (pH 7.5) and sucrose added to increase the osmolarity for injections. The final concentrations were 0.42 mM (1 mg/mL) AXT107, 1.26 mM total sulfo-SBED, 5 mM Tris-HCl, and 5% sucrose. For labeling SP2048, the sulfo-SBED reagent and SP2048 were dissolved in water and combined at a ratio of 3 to 1 (3 mM and 1 mM respectively). The mixture was then incubated for 2h at room temperature before being quenched with excess Tris-HCl (pH 7.5) and diluted to the desired concentration using Endothelial Base Medium (Lifeline Cell Technology, Frederick, MD). Final concentrations were 0.5 mM SP2048, 1.5 mM total sulfo-SBED, 6 mM Tris-HCl, and 49% (v/v) media.

Crosslinking and western blotting

Direct interactions of AXT107 with integrins was assessed *in vivo* using the sulfo-SBED labeled AXT107 in the OIR mouse model. A detailed procedure of the rearing and treatment of these mice can be found above. In total, one set of seven mice reared in room air and two sets of seven OIR mice were used in this study. After 24h of exposure to 1 μg sulfo-SBED AXT107 in both eyes, mice were euthanized, and the retinas excised and transferred to cold PBS in a 6-well culture plate. Once all retinas were collected, the plate was exposed to UV light, uncovered for 15 min at 365 nm. The retinas from each set (14 total) were pooled together in 1 mL of retina lysis buffer (50 mM Tris-HCl, pH 7.5; 2 mM EDTA; 150 mM NaCl; 1% Triton X-100; 0.1% SDS; 1% NP-40 with complete Protease Inhibitor Cocktail (Roche) in a 1.5 mL microcentrifuge tube and lysed using microcentrifuge tube pestles. The lysate then removed, taking care to avoid large debris, split into 0.25 mL aliquots and stored at −20°C.

For pulldowns, samples were thawed and a 50 μL sample was taken and labeled as "input". The remaining 200 μL was then incubated with 10 μL streptavidin-coated Sepharose beads (Cell Signaling Technologies, Danvers, MA) for 2h with end over end mixing at 4°C. After 2h, the beads were pelleted by centrifugation (11,000 × g) for 30 s and the supernatant saved as "flowthrough". The bead pellet was then washed with 0.5 mL retinal lysis buffer four times with pelleting by centrifugation between each wash. After the last wash the supernatant was discarded, and the bead pellet saved as the "pulldown" sample. The input, flowthrough, and pulldown samples where then mixed with 3× Blue Loading Buffer containing DTT (Cell Signaling Technologies, Danvers, MA) to a final concentration of 1× Blue Loading Buffer and 42 mM DTT and boiled for 5 min. The samples were then resolved by SDS-PAGE and the presence of integrins detected by western blot using the following primary antibodies: integrin α5, integrin αv, integrin β1, integrin β3, and β-tubulin and HRP-conjugated goat anti-rabbit or goat anti-mouse secondary antibodies. Images were collected using the iBright FL1000 imager.

HUVECs were seeded on 6-well plates coated with 10 μg/mL FN1 in endothelial growth media and cultured to confluency. Once confluent, the growth media was removed by vacuum and the cells washed two times with DPBS with calcium and magnesium and one time with endothelial base media. Sulfo-SBED labeled SP2048 (as prepared above) was then diluted to 100 μM in endothelial base media and 1 mL added to each well. The treated wells were incubated for 1.5 h at 37 °C and then crosslinked by exposure to 365 nm UV light for 15 min uncovered. The media was then removed by vacuum, the cells washed two times with DPBS with calcium and magnesium, and each well lysed in 0.5 mL retinal lysis buffer. The lysate was collected using cell scrapers and analyzed by pulldown and western blotting as described with AXT107 above.

QUANTIFICATION AND STATISTICAL ANALYSIS

Mouse images were obtained using SPOT RT 4.6 (Diagnostic Instruments Inc.) software and cell images were obtained using Infinity Capture v. 6.5.6 (Teledyne Lumenera) or Zen (Zeiss) software. Where indicated, western blots were quantified by densitometry using ImageJ software (NIH). No statistical analyses were performed. The number of mice (n) in each experiment is shown in the figure legends.

Ethics statement

Mice were treated in accordance with the Association for Research in Vision and Ophthalmology Guidelines regarding the care and use of animals in research. All animal studies were approved by the IACUC of Johns Hopkins University. Analysis of immunohistochemistry studies were performed by a masked observer and all experiments were done in duplicates and in some cases triplicates.